On the role of second gradient constitutive parameters in the static and dynamic analysis of heterogeneous media with micro-inertia effects

M. Ayad, N. Karathanasopoulos, H. Reda, J.F. Ganghoffer, H. Lakiss

On the role of second gradient constitutive parameters in the static and dynamic analysis of heterogeneous media with micro-inertia effects

M. Ayad[a,c], N. Karathanasopoulos[b], H. Reda [a] , J.F. Ganghoffer [c], H. Lakiss [a]

[a] Faculty of Engineering, Section III, Lebanese University, Campus Rafic Hariri, Beirut, Lebanon

[b] Chair of Computational Modeling of Materials in Manufacturing, ETH Zurich, Tannenstrasse 3, CH-8092, Switzerland

[c] LEM3, Université de Lorraine, CNRS. 7 rue Félix Savart, 57073, Metz, France

Abstract

In the current work, we develop a higher gradient dynamic homogenization method with micro-inertia effects. To that scope, we compute the macroscopic constitutive parameters up to the second gradient, using two distinct approaches, namely the Hamilton's principle and the total internal energy formulation. Thereupon, we analyze the sensitivity of the second gradient constitutive terms on the inner material and geometric parameters for the case of composite materials with a periodic, layered microstructure. The results suggest that the significance of the second gradient terms highly depend on the differences in the geometric and material properties of the underlying microstructural phases, as well as on the deformation mode of interest. What is more, the wave propagation study indicates that different higher gradient results are obtained, depending on the formulation used and on the wavenumber range of interest. In particular, Hamilton based, second gradient models perform poorly in the low wavenumber range, compared to first gradient or to analytic, exact solutions. Contrariwise, second gradient macroscopic constitutive formulations derived using the total higher gradient internal energy outperform first gradient approaches, better approximating the wave propagation characteristics of the effective medium, as the corresponding comparison in between the frequency diagrams and phase and group velocities suggest.

Keywords: micro-inertia, wave propagation, higher gradient, frequency

1. Introduction

It is experimentally proven that materials with a heterogeneous microstructure exhibit a dispersive wave propagation behavior, that is, each wavenumber travels with a different phase velocity (Erofeyev, 2003). However, homogenization models based on the classical, Cauchy-type elasticity theory are not able to reproduce different aspects of the physical behavior of heterogeneous media, such as wave dispersion.

The impact of the heterogeneous microstructure on the wave propagation characteristics of materials was first recognized and analyzed by Mindlin (1964), who proposed several non-local continuum models to capture the dispersion relation of planar waves. Since the early works in the 1960s by Toupin (1962) and Koiter (1969), there has been several literature contributions to the topic, recently summarized in (Askes and Aifantis, 2009). Generalized continuum theories offer an attractive alternative for capturing dynamic behaviors overlooked by classical elasticity, especially dispersion relations (Lombardo and Askes, 2012). In order to study low frequency wave propagation in effective continuum media, enriched second gradient elasticity descriptions have been developed which account for microstructural effects descriptive of the dispersive wave behavior (Aifantis, 1998). Gradient-enriched theories can sufficiently capture dynamic behaviors overlooked by classical elasticity, in which second gradient terms are neglected. Different theories based on an enrichment of the classical elasticity framework by higher order gradients have been proposed in the past to overcome deficiencies of classical elasticity (see Aifantis, 1992,1998;Askes and Aifantis 2009, Reda et al. 2018a) and plasticity (see Askes et al., 2002; Askes et al., 2008; Askes and Aifantis, 2011; Askes et al.,2012). Their formulation has aimed at describing both static and dynamic phenomena (Gutkin and Aifantis, 1999; Gourgiotis and Georgiadis, 2009; Gonella and Ruzzene, 2010; Gonella et al., 2011).

Applications of gradient elasticity in dynamics have fostered extensive research (Ostoja-Starzewki, 2002; Papargyri-Beskou, 2004; Andrianov, 2010; Askes and Aifantis, 2011). Gradient elasticity models are useful to predict the wave dispersion characteristics in heterogeneous or discrete systems (see Mindlin, 1964; Muhlhaus and Oka, 1996; Gonella et al., 2011, Gonella and Ruzzene, 2010, Alibert, 2015). A thorough analysis of the effects brought about by gradient elasticity models can be found in (Papargyri-Beskou et al., 2009; Fafalis et al., 2012), especially the impact of the higher-order inertial terms (see Metrikine and Askes, 2002; Askes and Aifantis, 2009; Askes et al., 2002). A detailed comparison between the dispersive characteristics of various simplified models of gradient elasticity can be found in (Askes et al., 2008). Accordingly, differences in between classical elasticity considerations and formulations that account for the role of higher order inner

material kinematics or non-finite strains can be found in (Reda et al. 2018b, Karathanasopoulos et al., 2019, Reda et al. 2018c)

The descriptions of microstructural effects analyzed in wave propagation are most of the time phenomenological in nature, following either the line of micromorphic models (see Berezovski et al., 2013) or second gradient continuum models (see Fafalis et al., 2012). The phenomenological nature of these models entails that the material parameters involved in the wave propagation formulations need to be calibrated to experiments, and consequently such models are not predictive. The large number of intrinsic parameters to be identified requires a somewhat difficult measurement protocol; this issue is addressed especially in (Polyzos et al., 2015; Iliopoulos et al., 2016; Réthoré et al., 2015).

In order to circumvent this drawback, multiscale methods have been developed to link the dispersive aspects of wave propagation to the microstructure of the material. Amongst these, homogenization techniques derive the dynamical macroscopic behavior by upscaling the microscopic one, so obtaining a more coarse description of the dispersive wave propagation features, but still reflecting in a predictive manner the impact of the underlying material microstructure.

Amongst the employed micromechanical methods, asymptotic homogenization is quite appealing and has developed importantly in the field of wave propagation over the last decade, (see Fish and Chen., 2001; Guenneau et al., 2013; Bacigalupo and Gambarotta, 2010, 2012, 2014 a,b). Boutin and Auriault (1993), extending the approach developed by Bensoussan et al. (1978), Sanchez-Palencia (1980) and Bakhvalov and Panasenko (1984), have proposed the long wave propagation in periodic media based on homogenization. The asymptotic expansion of the displacement field includes terms up to the third order to describe wave scattering. Homogenization in the time domain has also been proposed by several authors, see e.g. (Chen and Fish, 2000; Vivar-Pérez et al., 2009), considering both fast and slow time scales. In many studies, gradient elasticity theories have been derived from the continualisation of the response of a discrete lattice consisting of discrete masses and springs, see for example the early work of Mindlin (1972). Note that one of the biggest challenges of gradient elasticity theories is a physical interpretation of the involved length-scale parameters as a function of the given microstructure (Askes and Aifantis, 2011).

Resorting to computational approaches, finite element computations over the unit cell with periodic Bloch boundary conditions have been performed to model acoustic waves scattering and to evaluate the band structure (Hussein, 2009; Huang, 2011). As an alternative strategy for the solution of the Floquet-Bloch problem, plane wave expansions of the displacement vector, elastic moduli and mass are done in Fourier series with respect to the periodicity vectors (Nemat-Nasser et al., 2011-2012). This approach has the advantage to furnish exact dispersion relations.

Since the aforementioned approaches restrict to the low frequency range, they cannot describe the high frequency features encountered for microstructured periodic materials, like the presence of band gaps or negative refraction. High frequency behaviors were investigated in both discrete materials and composites with a high contrast of their elastic properties using asymptotic expansion methods (Andrianov et al., 2008, 2011; Craster et al., 2010; Zhikov (2000), Smyshlyaev (2009), Auriault and Boutin, 2012). First strain gradient formulations such as the ones elaborated in Mindlin (Mindlin 1964,1965) have further interest due to the possibility of associating them to higher order inertia terms, where the kinetic energy depends on the velocity gradient. These effects allow to better describe strain singularities at sharp crack tips and to capture size effects within the dynamic material behavior (dispersion relations) manifested by real materials such as porous materials, polymer foams (see Mindlin, 1964; Askes and Aifantis,2011). In the same spirit, a continuum model of Cauchy type including micro-inertia terms in the kinetic and potential energy was proposed in Wang and Sun (2002) and Sun and Huang (2007) with applications to the computation of the dispersion diagram for laminates which is compared with the exact solution for laminated media (Sun et al., 1968) obtained by the elasticity theory. The exact solution has been proved experimentally in (Robinson and al., 1974), where the existence of propagating bands and gaps in layered media was experimentally demonstrated.

A homogenization method for the analysis of wave propagation in materials with a periodic microstructure has been developed in Bacigalupo and Gambarotta (2012). The method is based on suitable micro-fluctuation functions which represent the material microstructure, incorporated in a variational-asymptotic approach. This approach has been recently extended in (Bacigalupo and Gambarotta, 2014a,b) to a higher order asymptotic expansion of the inner inertia terms, based on the mathematical convergence of the asymptotic solution (Smyshlyaev and Cherednichenko, 2000), though with first order macroscopic constitutive parameters. However, up to now, the significance of higher order macroscopic terms in the static and wave propagation analysis of microstructured media with micro-inertia effects has not been analyzed. As a result, the corresponding macroscopic higher gradient internal length parameters have not been evaluated, while their effect on the wave propagation attributes of microstructured media remains unknown.

In the current work, we develop a dynamic second gradient constitutive formulation for the analysis of the static and dynamic properties of heterogeneous media with micro-inertia effects. To that scope, we make use of the Hill-Mandel principle to relate macroscopic to microscopic parameters (Section 2), which we use as a basis for the derivation of the macroscopic equation of motion using separately the Hamilton's principle (Section 3.1.1) and the higher gradient description of the media's total internal energy (Section 3.1.2). We subsequently identify the micromechanical

constants relating micro-scale attributes with macro-scale mechanics in the case of longitudinal and transverse deformations of layered two-phase composite materials (Sections 3.1.1, 3.1.2). Thereafter, we analyze the significance of the higher gradient constitutive parameters as a function of the geometric and material properties of the underlying micro-structure in the static case (Section 3.1.3). We extend our analysis in the wave propagation regime, computing phase and group velocities and comparing the Hamilton and the higher gradient energy method results with already available literature results in Sections 3.2.1 and 3.2.2 accordingly. We discuss on the obtained results as a function of the method and wave number interest region in Section 4 and conclude in Section 5.

2. Homogenization methods

2.1 Second gradient mechanics and Hill-Mandel principle

We consider a representative volume element (RVE) of a heterogeneous medium occupying a domain Ω. The RVE is assumed to be small compared to the overall dimensions of the medium. We write the dynamic equilibrium of motion, as follows:

$$\sigma_{ij,j} = \rho \ddot{u}_i \tag{1}$$

where σ in Eq. (1) stands for the micro-stress developed within the RVE and u for the micro-displacement.

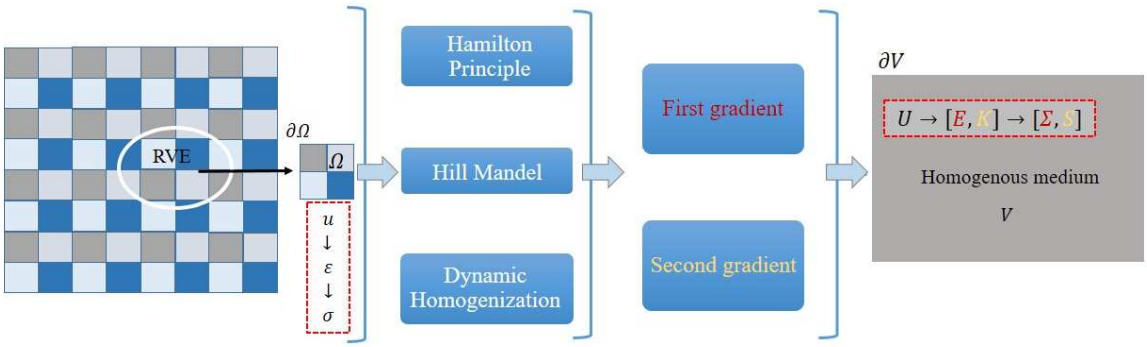

Figure 1: Homogenization concept from micro to macro model

We subsequently define the first and second order macro strain tensors E_{ij} and K_{ijk} and the first and second order stress tensors Σ_{ij} and S_{ijk} in component format accordingly, as follows (Trinh, 2011):

$$E_{ij} = \frac{1}{|\Omega|}\int_{\Omega} \varepsilon_{ij} d\Omega = \langle \varepsilon_{ij} \rangle = E_{ij} = \frac{1}{2}\left(\frac{\partial U_i}{\partial X_j} + \frac{\partial U_j}{\partial X_i} \right)$$
$$K_{ijk} = \frac{1}{|\Omega|}\int_{\Omega} \left(\varepsilon_{ij} \otimes \nabla_k \right) d\Omega = \langle \varepsilon_{ij} \otimes \nabla_k \rangle = \frac{1}{2}\left(\frac{\partial^2 U_i}{\partial X_j \partial X_k} + \frac{\partial^2 U_j}{\partial X_i \partial X_k} \right) \quad (2)$$
$$\Sigma_{ij} = \frac{1}{|\Omega|}\int_{\Omega} \sigma_{ij} d\Omega = \langle \sigma_{ij} \rangle, \qquad S_{ijk} = \langle \sigma_{ij} \otimes x_k \rangle$$

where the bracket notation $\langle . \rangle$ used in Eq. (2) denotes volume averages over the RVE of volume $|\Omega|$. The micro and macro scale position vectors are denoted with labels *x* and *X* respectively, while the lower and upper scale notations *u* and *U* are used for the micro and macro displacement components. We write the micro-displacement on the domain boundary as a function of the first and of the second order strain gradient terms of Eq. (2), as follows (Trinh et al., 2012):

$$u_i = x_j E_{ij} + \frac{1}{2} K_{ijk} x_j x_k \text{ on } \partial\Omega \quad (3)$$

We subsequently compute the difference between the average of the microscopic energy and macroscopic strain energy by writing the following identity resulting from (3):

$$\int_{\partial\Omega} \left(u_i - x_j E_{ij} - \frac{1}{2} K_{ijk} x_j x_k \right) (\sigma_{mi} - \Sigma_{mi}).n_m ds = 0 \quad (4)$$

Using the divergence theorem, we simplify Eq. (4) (the calculation is detailed in **Appendix A**), relating macroscopic and averaged microscopic energy terms with micro-inertia components as follows:

$$E_{ij}\Sigma_{ij} + K_{ijk} S_{ijk} = \langle \varepsilon_{ij} \sigma_{ij} \rangle + \left\langle \rho \ddot{u}_i \left(u_i - E_{ij} x_j - \frac{1}{2} K_{ijk} x_j x_k \right) \right\rangle \quad (5)$$

The linearity of the problem allows to introduce the localization operators relating the microscopic displacement $u_i(x,y)$ and strain $\varepsilon_{ij}(x,y)$ to the macro-strain components, as follows:

$$u_i(X,x) = H^E{}_{ijk}(x) E_{jk}(X) + H^K{}_{ijkl}(x) K_{jkl}(X)$$
$$\varepsilon_{ij}(X,x) = A^E{}_{ijkl}(x) E_{kl}(X) + A^K{}_{ijklm}(x) K_{klm}(X) \quad (6)$$

where $H^E(x), H^K(x)$ in Eq. (6) stand for the localizations tensors relating micro displacements to the first and second gradient strain tensors $E(X)$ and $K(X)$ respectively. Accordingly, $A^E(x), A^K(x)$ represent the localizations tensors relating the micro strains to the first and second gradient strain tensors $E(X)$ and $K(X)$. By definition of the homogenized constitutive law, the average stress and hyper stress tensors are evaluated as the variation of the internal energy in function of first and second gradient macro-deformation to obtain the following:

$$\begin{aligned} \Sigma_{ij}^{dyn} &= C_{ijdl}^{\hom} E_{dl} + B_{ijrst}^{\hom} K_{rst} \\ S_{ijk}^{dyn} &= D_{ijkdl}^{\hom} E_{dl} + A_{ijkrst}^{\hom} K_{rst} \end{aligned} \tag{7}$$

Where $C_{ijdl}^{\hom}$, $B_{ijrst}^{\hom}$, $D_{ijkdl}^{\hom}$ and $A_{ijkrst}^{\hom}$ are the first order, the coupling between the first and the second order stiffness tensors respectively, while Σ_{ij} and S_{ijk} stand accordingly for the Cauchy and for the hyperstress tensor.

In the sequel, we use Eq. (5) along with the Hamilton's principle to derive the dynamic equation of motion accounting for micro inertia terms.

2.2 Hamilton principle based second gradient mechanics

In order to derive the macro equation of motion we use Hamilton's principle, as follows:

$$\delta \iint_{V,t} (T - P)\, dV dt = \iint_{\partial V,t} Q_i \delta U_i dS dt \tag{8}$$

where V in Eq. (7) stands for the volume, Q_i for the traction exerted on the boundary of the volume V, and P and T are the deformation and kinetic energy densities respectively. The deformation energy density is defined as :

$$P = \frac{1}{2}\left\langle \varepsilon_{ij}\sigma_{ij} \right\rangle, T = \frac{1}{2}\left\langle \rho \dot{u}_i \dot{u}_i \right\rangle \tag{9}$$

Using Eq. (5) we write the expressions of deformation energy as a function of the macroscopic strains and of the micro-inertia components, as follows:

$$\begin{aligned} P &= \frac{1}{2} E_{ij}\Sigma_{ij} + \frac{1}{2} K_{ijk} S_{ijk} + P' \\ P' &= -\frac{1}{2}\left\langle \rho \ddot{u}_i \left(u_i - E_{ij}x_j - \frac{1}{2} K_{ijk} x_j x_k \right) \right\rangle = P'\left(E, \ddot{E}, K, \ddot{K}\right) = P'\left(E, \ddot{E}, \nabla E\right) \end{aligned} \tag{10}$$

where P' represents the deformation energy part related to micro-inertia terms .Accordingly, we write the kinetic energy part as a function of the macro-displacement components and mixed macroscopic displacement and microscopic fluctuation displacement term $\hat{u}_i$ terms contained in T', as follows:

$$T = \frac{1}{2}\langle \rho \dot{u}_i \dot{u}_i \rangle = \frac{1}{2}\langle \rho \dot{U}_i \dot{U}_i \rangle + T' \tag{11}$$

where T' in Eq. (11) relates to microscopic and higher gradient strain terms, as shown in the sequel. In particular, in order to derive an explicit form of T', we decompose the local displacement in the RVE into a displacement linear in the imposed macroscopic strain U_i^0 as in (4) and a microscopic fluctuation term $\hat{u}_i$ as follows :

$$\begin{aligned} u_i &= U_i^0 + \hat{u}_i \quad \forall x \in \Omega \\ u_i &= U_i^0 = E_{ij} x_j + \frac{1}{2} K_{ijk} x_j x_k \quad \forall x \in \partial\Omega \end{aligned} \tag{12}$$

By substituting the displacement field of Eq. (12) in the kinetic energy expression of Eq. (11) we get the macro and the micro part of the kinetic energy, as follows:

$$T = \frac{1}{2}\langle \rho \dot{U}_i^0 \dot{U}_i^0 \rangle + \langle \rho (\dot{\hat{u}}_i) \dot{U}_i^0 \rangle + \frac{1}{2}\langle \rho (\dot{\hat{u}}_i)(\dot{\hat{u}}_i) \rangle \tag{13}$$

The first part in the kinetic energy definition, Eq. (13), defines the macroscopic kinetic energy and the second part the coupling between the macroscopic and microscopic components, while the last term stands for purely microscopic energy contributions. Note that, according to the micromechanics assumption, tensors E_{ij} and K_{ijk} are constant over the RVE. As a result, the average density of the kinetic energy of the region $\frac{1}{2}\langle \rho \dot{U}_i^0 \dot{U}_i^0 \rangle$ and the density of the macro kinetic energy, scalar $\frac{1}{2}\langle \rho \rangle \dot{U}_i \dot{U}_i$ are equal. Therefore, it follows from (13) the expansion of the macro and micro kinetic energy terms successively as:

$$\begin{aligned} T &= \frac{1}{2}\langle \rho \rangle \dot{U}_i \dot{U}_i + \langle \rho (\dot{\hat{u}}_i) E_{ij} x_j \rangle + \frac{1}{2}\langle \rho (\dot{\hat{u}}_i) K_{ijk} x_j x_k \rangle + \frac{1}{2}\langle \rho (\dot{\hat{u}}_i)(\dot{\hat{u}}_i) \rangle \\ T' &= \langle \rho (\dot{\hat{u}}_i) \dot{E}_{ij} x_j \rangle + \frac{1}{2}\langle \rho (\dot{\hat{u}}_i) \dot{K}_{ijk} x_j x_k \rangle + \frac{1}{2}\langle \rho (\dot{\hat{u}}_i)(\dot{\hat{u}}_i) \rangle = T'(\dot{E}_{ij}, \dot{K}_{ijk}) \end{aligned} \tag{14}$$

We next substitute into Eq. (8) the expression of deformation and kinetic energy to obtain the macro equation of motion:

$$\delta\iint_{V,t}\left(\frac{1}{2}\langle\rho\rangle\dot{U}_i\dot{U}_i+T'-\left(\frac{1}{2}E_{ij}\Sigma_{ij}+\frac{1}{2}K_{ijk}S_{ijk}+P'\right)\right)dVdt=0 \tag{15}$$

We simplify Eq. (15) using integration by parts of each component as detailed in Eqs. (A.5-A.18) of the **Appendix A**. Thereupon, we obtain the equation of motion which contains surface (S) and volume (V) integrals as follows:

$$\begin{aligned}
&\int\Sigma_{ij,j}\delta U_i\partial V-\int S_{ijk,jk}\delta U_i dV+\int\frac{\partial}{\partial X_j}\left(\frac{\partial P'}{\partial E_{ij}}\right)\delta U_i dV+\int\frac{\partial}{\partial X_j}\left(\frac{\partial^2}{\partial t^2}\left(\frac{\partial P'}{\partial\ddot{E}_{ij}}\right)\right)\delta U_i dV\\
&+\int\frac{\partial}{\partial X_j}\frac{\partial}{\partial t}\left(\frac{\partial T'}{\partial\dot{E}_{ij}}\right)\delta U_i dV-\int\frac{\partial^2}{\partial X_j\partial X_k}\left(\frac{\partial^2}{\partial t^2}\left(\frac{\partial P'}{\partial\ddot{K}_{ijk}}\right)\right)\delta U_i dV-\int\left(\frac{\partial^2}{\partial X_j\partial X_k}\left(\frac{\partial P'}{\partial K_{ij}}\right)\delta U_i dV\right)\\
&-\int\frac{\partial}{\partial X_j}\left(\frac{\partial}{\partial X_k}\left(\frac{\partial}{\partial t}\left(\frac{\partial T'}{\partial\dot{K}_{ijk}}\right)\right)\right)\delta U_i dV\\
&-S_1-S_{2a}-S_{2b}+S_3-S_{4a}-S_{4b}-S_{4c}-S_{4d1}-S_{4d2}+S_{5a}+S_{5b}=\int\langle\rho\rangle\delta U_i\ddot{U}_i dV
\end{aligned} \tag{16}$$

Where the scalars S_i therein are surface integrals, detailed in the **Appendix A**. Separating the volume integrals from the surface integrals (S) in Eq. (16), we obtain the following macroscopic equation of motion:

$$\Sigma_{ij,j}-S_{ijk,kj}+F_i=\langle\rho\rangle\ddot{U}_i \tag{17}$$

where in Eq. (17) the Cauchy and the hyperstress tensors are calculated in the static situation (following the Hamilton principle formulation [Wang and Sun, 2006]), as follows:

$$\begin{aligned}
\Sigma_{ij}&=\frac{1}{2}\left\langle A^E_{krij}C_{krmn}A^E_{mndl}+A^E_{rsdl}.C_{rsmn}.A^E_{mnij}\right\rangle E_{dl}+\frac{1}{2}\left\langle A^E_{klij}C_{klmn}A^K_{mnrst}+A^K_{klrst}C_{klmn}A^E_{mnij}\right\rangle K_{rst}\\
S_{ijk}&=\frac{1}{2}\left\langle A^E_{rsdl}C_{rsmn}A^K_{mnijk}+A^K_{rsijk}C_{rsmn}A^E_{mndl}\right\rangle E_{dl}+\frac{1}{2}\left\langle A^K_{pfijk}C_{pfmn}A^K_{mnrst}+A^K_{dlrst}C_{dlmn}A^K_{mnijk}\right\rangle K_{rst}
\end{aligned} \tag{18}$$

In the Hamilton formulation of Eq. (17), the dynamic part is contained in the effective body force term F_i defined as follows (it does not depend on the constitutive law):

$$F_i=\frac{\partial}{\partial X_j}\left(\left(\frac{\partial P'}{\partial E_{ij}}\right)+\frac{\partial^2}{\partial t^2}\left(\frac{\partial P'}{\partial\ddot{E}_{ij}}\right)+\frac{\partial}{\partial t}\left(\frac{\partial T'}{\partial\dot{E}_{ij}}\right)+\frac{\partial}{\partial X_k}\left(-\left(\frac{\partial^2}{\partial t^2}\left(\frac{\partial P'}{\partial\ddot{K}_{ijk}}\right)\right)\right)-\frac{\partial}{\partial t}\left(\frac{\partial T'}{\partial\dot{K}_{ijk}}\right)-\left(\frac{\partial P'}{\partial K_{ijk}}\right)\right) \tag{19}$$

The micro-inertia force of Eq. (19) is calculated as a function of the displacement and strain localization operators introduced in Eq. (6) as follows:

$$F_i = \frac{\partial}{\partial X_j}\left(\frac{1}{2}\ddot{E}_{mn}\left\langle\rho\left(H^E_{imn}x_j + H^E_{mij}x_n - 2\delta^m_i x_j x_n\right)\right\rangle + \frac{1}{2}\ddot{K}_{rsk}\left\langle\rho\left(H^K_{irsk}x_j + \frac{1}{2}H^E_{rij}x_s x_k - \delta^r_i x_s x_j x_k\right)\right\rangle\right)$$
$$-\frac{\partial^2}{\partial X_j \partial X_k}\left(\ddot{E}_{rs}\left\langle\frac{\rho}{2}\left(H^K_{rijk}x_s + \frac{1}{2}H^E_{irs}x_j x_k - \delta^p_i x_s x_j x_k\right)\right\rangle + \frac{1}{4}\ddot{K}_{rst}\left\langle\rho\left(H^K_{rijk}x_s x_t + H^K_{irst}x_j x_k - \delta^r_i x_s x_j x_k x_t\right)\right\rangle\right) \quad (20)$$

In the sequel, we derive the dynamic equilibrium based on the total higher gradient potential energy in the presence of micro-inertia effects.

2.1.2 Dynamic higher gradient energy formulation of the constitutive law

In the Dynamic Higher Gradient Energy (DHGE) formulation, we compute the effective dynamic constitutive law by deriving the expression of the internal energy. Inserting the localization tensors of Eq. (6) back into Eq. (5) enables to write the total internal energy as a function of the macro-strain parameters in Eq. (21), as follows:

$$2.W^{\text{int}}(E,K) = \left(E_{ij}.\Sigma_{ij} + K_{ijk}.S_{ijk}\right) = \left\langle\varepsilon_{ij}\sigma_{ij}\right\rangle + \left\langle\rho\ddot{u}_i\left(u_i - E_{ij}x_j - \frac{1}{2}K_{ijk}x_j x_k\right)\right\rangle$$
$$= \left\langle A^E_{ijkl}E_{kl}.C_{ijmn}.A^E_{mnrs}.E_{rs} + A^E_{ijkl}.E_{kl}C_{ijmn}A^K_{mnrst}K_{rst} + A^K_{ijklf}K_{klf}C_{ijmn}A^E_{mnrs}E_{rs} + A^K_{ijklf}K_{klf}C_{ijmn}A^K_{mnrst}K_{rst}\right\rangle$$
$$+\left\langle\rho\begin{pmatrix} H^E_{ijk}\ddot{E}_{jk}H^E_{iqr}E_{qr} + H^E_{ijk}\ddot{E}_{jk}H^K_{irst}K_{rst} - H^E_{ijk}\ddot{E}_{jk}E_{iq}x_q - \frac{1}{2}H^E_{ijk}\ddot{E}_{jk}K_{iqr}x_q x_r \\ +H^K_{ijkl}\ddot{K}_{jkl}H^E_{iqr}E_{qr} + H^K_{ijkl}\ddot{K}_{jkl}H^K_{irst}K_{rst} - H^K_{ijkl}\ddot{K}_{jkl}E_{iq}x_q - \frac{1}{2}H^K_{ijkl}\ddot{K}_{jkl}K_{iqr}x_q x_r \end{pmatrix}\right\rangle \quad (21)$$

The first order macro stress tensor and the second gradient tensor are obtained by deriving the expression of the energy (Eq. (21)) with respect to the macro-deformation of the first and of the second gradient respectively (the derivations are detailed in **Appendix B**):

$$
\begin{aligned}
\Sigma^{dyn}{}_{ij} &= \frac{\partial W^{\text{int}}(E,K,\ddot{E},\ddot{K})}{\partial E_{ij}} + \frac{\partial^2}{\partial t^2}\left(\frac{\partial W^{\text{int}}(E,K,\ddot{E},\ddot{K})}{\partial \ddot{E}_{ij}}\right) \\
&= E_{dl}\left\langle \frac{1}{2}\left(A^E_{krij}C_{krmn}A^E_{mndl} + A^E_{rsdl}.C_{rsmn}.A^E_{mnij}\right)\right\rangle + K_{rst}\left\langle \frac{1}{2}\left(A^E_{klij}C_{klmn}A^K_{mnrst} + A^K_{klrst}C_{klmn}A^E_{mnij}\right)\right\rangle \\
&\quad + \ddot{E}_{dl}\left\langle \frac{\rho}{2}\left(H^E_{qdl}H^E_{qij} + H^E_{kij}H^E_{kdl} - H^E_{idl}x_j - H^E_{dij}x_l\right)\right\rangle + \\
&\quad \ddot{K}_{rst}\left\langle \frac{\rho}{2}\left(H^K_{qrst}H^E_{qij} + H^K_{krst}H^E_{kij} - H^K_{irst}x_j - \frac{1}{2}H^E_{rij}x_s x_t\right)\right\rangle \\
S_{ijk} &= \frac{\partial W^{\text{int}}(E,K,\ddot{E},\ddot{K})}{\partial K_{ijk}} + \frac{\partial^2}{\partial t^2}\frac{\partial W^{\text{int}}(E,K,\ddot{E},\ddot{K})}{\partial \ddot{K}_{ijk}} \\
&= \left\langle \frac{1}{2}A^E_{rsdl}C_{rsmn}A^K_{mnijk} + \frac{1}{2}A^K_{rsijk}C_{rsmn}A^E_{mndl}\right\rangle.E_{dl} + \left\langle \frac{1}{2}A^K_{pfijk}C_{pfmn}A^K_{mnrst} + \frac{1}{2}A^K_{dlrst}C_{dlmn}A^K_{mnijk}\right\rangle.K_{rst} \\
&\quad + \left\langle \frac{\rho}{2}\left(H^E_{qdl}H^K_{qijk} + H^E_{rdl}H^K_{rijk} - \frac{1}{2}H^E_{idl}x_k x_j - H^K_{dijk}x_l\right)\right\rangle.\ddot{E}_{dl} + \\
&\quad \left\langle \frac{\rho}{2}\left(H^K_{lrst}H^K_{lijk} + H^K_{drst}H^K_{dijk} - \frac{1}{2}H^K_{rijk}x_s x_t - \frac{1}{2}H^K_{irst}x_j x_k\right)\right\rangle.\ddot{K}_{rst}
\end{aligned}
\tag{22}
$$

We note that the dynamic part in the macroscopic constitutive expressions in Eq. (22) arises from the derivation of the micro-inertia terms with respect to the tensors $\ddot{E}$ and $\ddot{K}$. Considering a plane harmonic wave solution $\left(U = U_0 e^{I\cdot(k\cdot X_1 - wt)}\right)$, the second time derivative of the strain and strain gradient are expressed as follows:

$$
\begin{pmatrix} \ddot{E} \\ \ddot{K} \end{pmatrix} = -w^2 \begin{pmatrix} E \\ K \end{pmatrix} \tag{23}
$$

where *w* in Eq. (23) is the frequency of the propagating waves. Using Eq. (22), we express the homogenized dynamic constitutive tensors in Eq. (7), as follows (**Appendix B**):

$$
\begin{aligned}
C_{ijdl}^{\hom,dyn} &= \left\langle \frac{1}{2}\left(A_{krij}^{E} C_{krmn} A_{mndl}^{E} + A_{rsdl}^{E} . C_{rsmn} . A_{mnij}^{E} \right) \right\rangle - w^2 \left\langle \frac{\rho}{2} \begin{pmatrix} H_{qdl}^{E} H_{qij}^{E} + H_{kij}^{E} H_{kdl}^{E} \\ -H_{idl}^{E} x_j - H_{dij}^{E} x_l \end{pmatrix} \right\rangle \\
B_{ijrst}^{\hom,dyn} &= \left\langle \frac{1}{2}\left(A_{klij}^{E} C_{klmn} A_{mnrst}^{K} + A_{klrst}^{K} C_{klmn} A_{mnij}^{E} \right) \right\rangle - w^2 \left\langle \frac{\rho}{2} \begin{pmatrix} H_{qrst}^{K} H_{qij}^{E} + H_{krst}^{K} H_{kij}^{E} \\ -H_{irst}^{K} x_j - \frac{1}{2} H_{rij}^{E} x_s x_t \end{pmatrix} \right\rangle \\
D_{ijkdl}^{\hom,dyn} &= \left\langle \frac{1}{2} A_{rsdl}^{E} C_{rsmn} A_{mnijk}^{K} + \frac{1}{2} A_{rsijk}^{K} C_{rsmn} A_{mndl}^{E} \right\rangle - w^2 \left\langle \frac{\rho}{2} \begin{pmatrix} H_{qdl}^{E} H_{qijk}^{K} + H_{rdl}^{E} H_{rijk}^{K} \\ -\frac{1}{2} H_{idl}^{E} x_k x_j - H_{dijk}^{K} x_l \end{pmatrix} \right\rangle = B_{dlijk}^{\hom,dyn} \\
A_{ijkrst}^{\hom,dyn} &= \left\langle \frac{1}{2} A_{pfijk}^{K} C_{pfmn} A_{mnrst}^{K} + \frac{1}{2} A_{dlrst}^{K} C_{dlmn} A_{mnijk}^{K} \right\rangle - w^2 \left\langle \frac{\rho}{2} \begin{pmatrix} H_{lrst}^{K} H_{lijk}^{K} + H_{drst}^{K} H_{dijk}^{K} \\ -\frac{1}{2} H_{rijk}^{K} x_s x_t - \frac{1}{2} H_{irst}^{K} x_j x_k \end{pmatrix} \right\rangle
\end{aligned}
\tag{24}
$$

3. Results

3.1 Composite laminated media

We apply the previously elaborated methodologies to the case of composite materials with a periodic, layered microstructure. To that scope, we define below the attributes of the unit-cell structure, its total length set to $L=1$. Fig. 2 summarizes the geometric parameters characterizing the unit-cell, as well as the material parameters for both two phases.

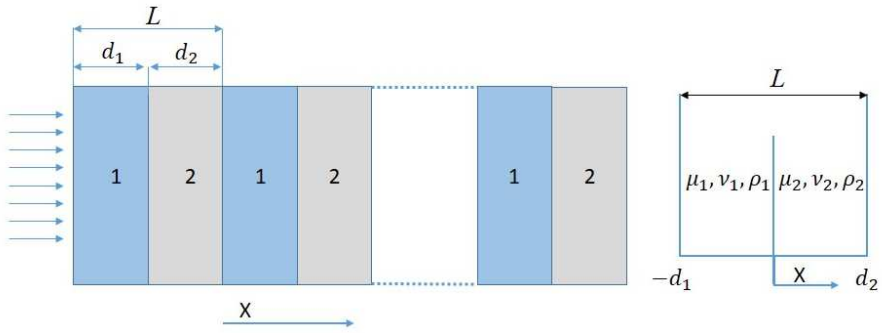

Figure 2: Periodic layered composite material geometry (left) and its unit cell material parameters (right)

In Fig. 2, μ_1, μ_2 and ν_1, ν_2 stand for the shear moduli and for the Poisson's ratio; ρ_1, ρ_2 and d_1, d_2 represent the mass density and the thickness of the first and of the second layers. The micro-displacement field is represented with superscripts for each medium and subscripts for the direction of each displacement component, as follows:

$$u^1 = \begin{bmatrix} u_1^1 \\ u_2^1 \end{bmatrix}, u^2 = \begin{bmatrix} u_1^2 \\ u_2^2 \end{bmatrix}$$

(25)

3.1.1 Identification of micromechanical constants upon normal deformations

We subsequently determine the expressions of the localization operators of Eq. (6) for the case of normal macroscopic deformations. In such a deformation mode, the macro displacement field is along the X direction, so that it holds:

$$U_1 = f(X_1) \Rightarrow E_{11} \neq 0,\ K_{111} \neq 0 \tag{26}$$

The micro-displacements follow the definition of Eq. (25) and (6), where the coefficients of the localization tensors are denoted with a_i and b_i for the first and second layer successively, as follows:

$$\begin{aligned}
& u_1^1(x) = \begin{bmatrix} H_{111}^{E\ 1} & H_{1111}^{K\ 1} \end{bmatrix} . \begin{bmatrix} E_{11} \\ K_{111} \end{bmatrix} = \begin{bmatrix} a_0 + a_1 x & a_2 + a_3 x + a_4 \dfrac{x^2}{2} \end{bmatrix} . \begin{bmatrix} E_{11} \\ K_{111} \end{bmatrix} \\
\Rightarrow & \begin{cases} \varepsilon_{11}^1(x) = \begin{bmatrix} A_{1111}^{E\ 1} & A_{11111}^{K\ 1} \end{bmatrix} . \begin{bmatrix} E_{11} \\ K_{111} \end{bmatrix} = \begin{bmatrix} a_1 & a_3 + a_4 x \end{bmatrix} . \begin{bmatrix} E_{11} \\ K_{111} \end{bmatrix} \\ \end{cases} \\
& u_1^2(x) = \begin{bmatrix} H_{111}^{E\ 2} & H_{1111}^{K\ 2} \end{bmatrix} . \begin{bmatrix} E_{11} \\ K_{111} \end{bmatrix} = \begin{bmatrix} b_0 + b_1 x & b_2 + b_3 x + b_4 \dfrac{x^2}{2} \end{bmatrix} . \begin{bmatrix} E_{11} \\ K_{111} \end{bmatrix} \\
\Rightarrow & \begin{cases} \varepsilon_{11}^2(x) = \begin{bmatrix} A_{1111}^{E\ 2} & A_{11111}^{K\ 2} \end{bmatrix} . \begin{bmatrix} E_{11} \\ K_{111} \end{bmatrix} = \begin{bmatrix} b_1 & b_3 + b_4 x \end{bmatrix} . \begin{bmatrix} E_{11} \\ K_{111} \end{bmatrix} \\ \end{cases}
\end{aligned} \tag{27}$$

Eq. (27) contains a total of 10 unknown parameters a_i and b_i. The micro-stress developed in each inner material phase is given as a function of the micro-strains of Eq. (27), as follows:

$$\begin{cases} \sigma_{11}^1(x) = \left(\lambda_1 + 2\mu_1\right) \cdot \varepsilon_{11}^1(x) = \left(\lambda_1 + 2\mu_1\right) \cdot \begin{bmatrix} a_1 & a_3 + a_4 x \end{bmatrix} . \begin{bmatrix} E_{11} \\ K_{111} \end{bmatrix} \\ \sigma_{11}^2(x) = \left(\lambda_2 + 2\mu_2\right) \cdot \varepsilon_{11}^2(x) = \left(\lambda_2 + 2\mu_2\right) \cdot \begin{bmatrix} b_1 & b_3 + b_4 x \end{bmatrix} . \begin{bmatrix} E_{11} \\ K_{111} \end{bmatrix} \end{cases} \tag{28}$$

where λ in Eq. (28) defines the first Lame coefficient, equal to $2\mu\nu/\left(1-2\nu\right)$. Using Eq. (2) we get $E_{11} = \dfrac{\partial U_1}{\partial x}, K_{111} = \dfrac{\partial^2 U_1}{\partial x^2}$ for the first and second gradient macro strains. We use the interface

continuity condition for the displacements, upon which we obtain 2 equations. Accordingly, using the boundary conditions for the displacement field, we retrieve 4 additional equilibrium equations, noting that first and second gradient terms E_{ij} and K_{ijk} can be treated independent. The body forces are null within the cell, so that the continuity of stresses and stress gradients provides us with a total of three additional equations (two and one respectively). The boundary and interface conditions are summarized as follows:

$$\begin{cases} u_1^1(0) = u_2^1(0) \\ u_1^1(-d_1) = -E_{11}d_1 + K_{111}\dfrac{d_1^{\,2}}{2}, u_2^1(d_2) = E_{11}d_2 + K_{111}\dfrac{d_2^{\,2}}{2} \\ \sigma_{11}^1(0) = \sigma_{11}^2(0), \dfrac{\partial \sigma_{11}^1}{\partial x}(0) = \dfrac{\partial \sigma_{11}^2}{\partial x}(0) \end{cases} \tag{29}$$

The 9 equations in the set of Eqs. (29) do however not suffice to calculate the 10 coefficients appearing in Eq. (27). As an additional condition, we require the average of the microscopic deformations for the first and second gradient to be equal to the corresponding macroscopic deformations, as follows:

$$\left\langle \varepsilon_{11} \right\rangle_\Omega = E_{11}, \left\langle \nabla \varepsilon_{11} \right\rangle_\Omega = K_{111} \tag{30}$$

Remark: note that we impose the quadratic displacement only to the RVE boundary and not in the entire volume; this entails that the average (in the volume sense) of the fluctuating displacement does vanish only on the RVE boundary but not necessarily within the whole volume. We use the condition that the average microscopic strains ε_{ij} and their gradient $\nabla_k(\varepsilon_{ij})$ are equal to the macroscopic strain E_{ij} and strain gradient K_{ijk} components respectively similarly to (Boutin, 1996), so that the fluctuation of the strain and strain gradient has zero mean values.

Note that Eq. (30) provides solely one additional dependent condition, as the average of micro-strains leads to a condition that is a linear combination of the ones contained in Eq. (29). Solving the system of Eqs. (29, 30) with the use of Eq. (27) and (28), we obtain the following expressions of the microscopic coefficients a_i and b_i :

$$a_0 = -\frac{d_1 d_2\left((\lambda_1+2\mu_1)-(\lambda_2+2\mu_2)\right)}{(\lambda_1+2\mu_1)d_2+d_1(\lambda_2+2\mu_2)}, a_1 = \frac{(\lambda_2+2\mu_2)(d_1+d_2)}{(\lambda_1+2\mu_1)d_2+d_1(\lambda_1+2\mu_1)},$$

$$a_2 = \frac{d_2 d_1\left((\lambda_1+2\mu_1)^2 d_2 d_1+(\lambda_1+2\mu_1)(\lambda_2+2\mu_2)\left(d_1^2-d_2 d_1+L d_1\right)+d_1 d_2(\lambda_2+2\mu_2)^2\right)}{2\left((\lambda_1+2\mu_1)d_2+d_1(\lambda_2+2\mu_2)\right)^2},$$

$$a_3 = -\frac{(\lambda_2+2\mu_2)\left(d_1(\lambda_2+2\mu_2)\left(d_1^2-d_2^2+L d_1\right)+d_2(\lambda_1+2\mu_1)\left(d_1^2+d_2 d_1\right)\right)}{2\left((\lambda_1+2\mu_1)d_2+d_1(\lambda_2+2\mu_2)\right)^2},$$

$$a_4 = \frac{(\lambda_2+2\mu_2)L}{(\lambda_1+2\mu_1)d_2+d_1(\lambda_2+2\mu_2)}$$

$$b_0 = -\frac{d_1 d_2\left((\lambda_1+2\mu_1)-(\lambda_2+2\mu_2)\right)}{(\lambda_1+2\mu_1)d_2+d_1(\lambda_2+2\mu_2)}, b_1 = \frac{(\lambda_1+2\mu_1)(d_1+d_2)}{(\lambda_1+2\mu_1)d_2+d_1(\lambda_2+2\mu_2)}, \quad (31)$$

$$b_2 = \frac{d_2 d_1\left((\lambda_1+2\mu_1)^2 d_2 d_1+(\lambda_1+2\mu_1)(\lambda_2+2\mu_2)\left(d_1^2-d_2 d_1+L d_1\right)+d_1 d_2(\lambda_2+2\mu_2)^2\right)}{2\left((\lambda_1+2\mu_1)d_2+d_1(\lambda_2+2\mu_2)\right)^2},$$

$$b_3 = -\frac{(\lambda_1+2\mu_1)\left(d_1(\lambda_2+2\mu_2)\left(L d_1-d_2^2+d_1^2\right)+d_2(\lambda_1+2\mu_1)\left(d_1^2+d_2 d_1\right)\right)}{2\left((\lambda_1+2\mu_1)d_2+d_1(\lambda_2+2\mu_2)\right)^2},$$

$$b_4 = \frac{(\lambda_1+2\mu_1)L}{(\lambda_1+2\mu_1)d_2+d_1(\lambda_2+2\mu_2)}$$

3.1.2 Identification of micromechanical constants upon transverse deformations

In the transverse deformation case, the displacement field is parallel to the direction of the layers, so that $U_2 = f(X_1) \Rightarrow E_{21} \neq 0, K_{211} \neq 0$. Writing the micro-displacements as a function of the macro-strain in each layer through the localization operators of Eq. (6), we obtain:

$$u_2^1(x_1) = \left[H_{212}^{E\ 1} \quad H_{2121}^{K\ 1}\right].\begin{bmatrix} E_{21} \\ K_{211}\end{bmatrix} = \begin{bmatrix} a_0+a_1 x_1 & a_2+a_3 x_1+a_4\dfrac{x_1^2}{2}\end{bmatrix}.\begin{bmatrix} E_{21} \\ K_{211}\end{bmatrix}$$

$$u_2^2(x_1) = \left[H_{212}^{E\ 2} \quad H_{2121}^{K\ 2}\right].\begin{bmatrix} E_{21} \\ K_{211}\end{bmatrix} = \begin{bmatrix} b_0+b_1 x_1 & b_2+b_3 x_1+b_4\dfrac{x_1^2}{2}\end{bmatrix}.\begin{bmatrix} E_{21} \\ K_{211}\end{bmatrix} \quad (32)$$

$$u_1^1(x_2) = u_1^2(x_2) = A x_2 E_{21} + C\frac{x_2^2}{2}K_{211} = \left[H_{121}^{E} \quad H_{1211}^{K}\right].\begin{bmatrix} E_{21} \\ K_{211}\end{bmatrix}$$

Eq. (32) contains a total of 12 unknowns. The micro-strains field and its gradient are computed using Eq. (32), as follows:

$$\varepsilon_{21}^{1}(x_1,x_2)=\frac{1}{2}\left(\frac{\partial u_2^1}{\partial x_1}(x_1)+\frac{\partial u_1^1}{\partial x_2}(x_2)\right)=\left[A_{2121}^{E\ 1}\quad A_{21211}^{K\ 1}\right]\begin{bmatrix}E_{21}\\K_{211}\end{bmatrix}$$
$$=\begin{bmatrix}\frac{1}{2}(a_1+A) & \frac{1}{2}(a_3+a_4x_1+Cx_2)\end{bmatrix}\begin{bmatrix}E_{21}\\K_{211}\end{bmatrix}$$
$$\varepsilon_{21,1}^{1}=\frac{1}{2}(a_4K_{211}),\varepsilon_{21,2}^{1}=\frac{1}{2}(CK_{211})$$
$$\varepsilon_{21}^{2}(x_1,x_2)=\frac{1}{2}\left(\frac{\partial u_2^2}{\partial x_1}(x_1)+\frac{\partial u_1^2}{\partial x_2}(x_2)\right)=\left[A_{2121}^{E\ 2}\quad A_{21211}^{K\ 2}\right]\begin{bmatrix}E_{21}\\K_{211}\end{bmatrix} \tag{33}$$
$$=\begin{bmatrix}\frac{1}{2}(b_1+A) & \frac{1}{2}(b_3+b_4x_1+Cx_2)\end{bmatrix}\begin{bmatrix}E_{21}\\K_{211}\end{bmatrix}$$
$$\varepsilon_{21,1}^{2}=\frac{1}{2}(b_4K_{211}),\varepsilon_{21,2}^{2}=\frac{1}{2}(CK_{211})$$

Since the first and second gradient micro-strains in Eq. (33) are symmetric tensors, we require that the localization tensors of Eq. (6) enjoy the following symmetry properties:

$$H_{212}^{E}=H_{221}^{E},H_{112}^{E}=H_{121}^{E}$$
$$A_{2121}^{E}=A_{1221}^{E},A_{21211}^{K}=A_{12211}^{K} \tag{34}$$

Using Eq. (33), we compute the micro-stress developed in each of the inner material phases, as follows:

$$\sigma_{21}^{1}(x_1,x_2)=2\mu_1\cdot\varepsilon_{21}^{1}(x_1,x_2)=2\mu_1\left(a_1E_{21}+a_3K_{211}+a_4x_1K_{211}+AE_{21}+Cx_2K_{211}\right)$$
$$\sigma_{21}^{2}(x_1,x_2)=2\mu_2\cdot\varepsilon_{21}^{2}(x_1,x_2)=2\mu_2\left(b_1E_{21}+b_3K_{211}+b_4x_1K_{211}+AE_{21}+Cx_2K_{211}\right) \tag{35}$$

where the first and second gradient macro-strain components entering Eq. (33) are defined as follows (Eq. (2)):

$$E_{21}=\frac{1}{2}\left(\frac{\partial U_2}{\partial X_1}+\frac{\partial U_1}{\partial X_2}\right),E_{11}=0,E_{22}=0$$
$$K_{211}=\frac{\partial E_{12}}{\partial X_1},K_{122}=0,K_{112}=0 \tag{36}$$

In order to calculate the constants a_i and b_i, we use the continuity conditions for the displacement at the interface, which provide two equations; the boundary conditions for the displacements provide 4 equations and the continuity of stress and stress gradients at the interface provide two and one equilibrium equation respectively. What is more, we use the average of the microscopic first gradient deformations and the average of the microscopic second gradient deformations to be equal to the corresponding macroscopic ones, as follows:

$$
\begin{aligned}
&u_2^1(0) = u_2^2(0) \\
&u_2^1(-d_1) = -E_{21}d_1 + K_{211}\frac{{d_1}^2}{2}, u_2^2(d_2) = E_{21}d_2 + K_{211}\frac{{d_2}^2}{2} \\
&\sigma_{21}^1(0) = \sigma_{21}^2(0), \frac{\partial \sigma_{21}^1}{\partial x_1}(0) = \frac{\partial \sigma_{21}^2}{\partial x_1}(0) \\
&\langle \varepsilon_{21} \rangle = E_{21}, \langle \varepsilon_{21,1} \rangle = K_{211}, \langle \varepsilon_{12,2} \rangle = K_{122}
\end{aligned}
\tag{37}
$$

Solving the system of Eq. (37) using Eq. (33)-(36), we obtain the following constants a_i and b_i for the transverse deformation mode:

$$
\begin{aligned}
a_0 &= \frac{d_1 d_2(\mu_1 - \mu_2)(d_1 + d_2 - 3L)}{L(d_1\mu_2 + d_2\mu_1)}, a_1 = \frac{(\mu_1 - \mu_2){d_2}^2 + ((-d_1 + 3L)\mu_2 + \mu_1(d_1 - 2L))d_2 + Ld_1\mu_2}{L(d_1\mu_2 + d_2\mu_1)} \\
a_2 &= \frac{d_2 d_1\left(\frac{d_2 d_1 {\mu_1}^2}{2} + \left(\frac{{d_1}^2}{2} + Ld_1 - d_2\left(L - \frac{d_2}{2}\right)\right)\mu_1\mu_2 + \frac{d_2 d_1 {\mu_2}^2}{2}\right)}{(d_1\mu_2 + d_2\mu_1)^2}, \\
a_3 &= -\frac{\mu_2\left(-{d_2}^3\mu_1 + (2L\mu_1 - d_1){d_2}^2 + \mu_1{d_1}^2 d_2 + 2\left(L + \frac{d_1}{2}\right){d_1}^2\mu_2\right)}{2(d_1\mu_2 + d_2\mu_1)^2} \\
a_4 &= \frac{2\mu_2 L}{(d_1\mu_2 + d_2\mu_1)}, b_0 = \frac{d_1 d_2(\mu_1 - \mu_2)(d_1 + d_2 - 3L)}{L(d_1\mu_2 + d_2\mu_1)}, \\
b_1 &= \frac{(-\mu_1 + \mu_2){d_1}^2 + ((-d_2 + 3L)\mu_1 + \mu_2(d_2 - 2L))d_2 + Ld_2\mu_1}{(d_1\mu_2 + d_2\mu_1)}, \\
b_2 &= \frac{d_2 d_1\left(\frac{d_2 d_1 {\mu_1}^2}{2} + \left(\frac{{d_1}^2}{2} + Ld_1 - d_2\left(L - \frac{d_2}{2}\right)\right)\mu_1\mu_2 + \frac{d_2 d_1 {\mu_2}^2}{2}\right)}{(d_1\mu_2 + d_2\mu_1)^2}, \\
b_3 &= -\frac{-{d_2}^3{\mu_1}^2 + (2L{\mu_1}^2 - d_1\mu_2\mu_1){d_2}^2 + {\mu_1}^2{d_1}^2 d_2 + (2L + d_1){d_1}^2\mu_2\mu_1}{2(d_1\mu_2 + d_2\mu_1)^2}, \\
b_4 &= \frac{2\mu_1 L}{(d_1\mu_2 + d_2\mu_1)}, A = \frac{2L - d_1 - d_2}{L}, C = 0
\end{aligned}
\tag{38}
$$

3.2 Homogenized higher gradient static effective properties

We subsequently analyze the higher gradient static effective properties of the layered media. The latter are independent of the method used for their derivation, as it can be observed by comparing the Hamilton principle expanded in section 2.1.1 (Eqs. (17-18)) and the internal energy method in section 2.1.2 (Eqs. (22)-(24)), $w = 0$).

3.2.1 Longitudinal mode

We compute the higher gradient constitutive properties of the layered composite of Section 3.1 for the case of identical elastic material properties $\left(\lambda_1=\lambda_2=\lambda,\mu_1=\mu_2=\mu\right)$, namely Lamé coefficient and shear modulus values used in the elastic law $\left(\sigma_{11}^{1,2}(x)=\left(\lambda_{1,2}+2\mu_{1,2}\right)\cdot\varepsilon_{11}^{1,2}(x)\right)$. After calculating the constants of the displacement vectors in each layer, we use Eq. (18) or the static part of Eq. (24) to calculate the homogenized tensors of first gradient elasticity, $C^{\hom}$ (in MPa), the coupling tensor $B^{\hom}, D^{\hom}$ (in $MPa\cdot m$) and the second gradient tensor $A^{\hom}$ (in $MPa\cdot m^2$) respectively, as a function of the geometric attributes of the unit-cell. In Eq. (39), we provide the corresponding expressions as a function of the layers thickness ratio $\alpha=d_1/d_2$ and of the total unit-cell length L of the cell, as follows:

$$
\begin{aligned}
&C_{1111}^{\hom}=\lambda+2\mu\\
&B_{11111}^{\hom}=D_{11111}^{\hom}=\frac{(\lambda+2\mu)}{2}\left(-\frac{\left(3\alpha^2-1\right)}{(\alpha+1)^2}\right)\cdot L\\
&A_{111111}^{\hom}=\frac{(\lambda+2\mu)}{3}\left(\frac{\left(7\alpha^4+\alpha^3-3\alpha^2+\alpha+1\right)}{(\alpha+1)^4}\right)\cdot L^2
\end{aligned}
\tag{39}
$$

For layers of identical properties, the set of Eqs. (39) provides a first gradient tensor $C_{1111}^{\hom}$ which is identical to the constitutive tensor of both layers. In Fig. 3a, we depict the homogenized tensors as a function of the geometrical ratio $\alpha=d_1/d_2$ for equal material moduli in each inner material phase.

What is more, we explore the sensitivity of the second gradient terms on the discrepancies of the inner material properties in the layered composite medium for the case of equal inner layer thickness $\left(d_1=d_2\right)$. Thereupon, we calculate the characteristic second gradient length $l_{e111}(m)$ as a function of the elastic modulus ratio $\phi=E_2/E_1$, plotted in Fig. 4a.

$$
l_{e111}=\sqrt{\frac{A_{111111}^{\hom}}{C_{1111}^{\hom}}}=0.72\cdot L\sqrt{\frac{(\phi^2+1.12\phi+0.322)(\phi^2+0.033\phi+0.041)}{(\phi+0.67)^3\phi}}
\tag{40}
$$

The characteristic length of Eq. (40) for equal layers thickness and for the first layer being 1.5 times the thickness of the second ($d_1=1.5d_2$) is recorded in Fig. 4a as a function of the elastic modulus

ratio ϕ . The results indicate that the effect of second gradient terms increase when the contrast in the material attributes of the microstructural phases increases.

3.2.2 Transverse mode

For the case of transverse deformations, we calculate the homogenized constitutive tensors for equal micro-scale material properties using Eq. (18) or Eq. (24) $(w=0)$, as a function of the layers thickness ratio $\alpha=d_1/d_2$, to be:

$$
\begin{aligned}
&C^{\text{hom}}_{2121} = 2\mu \\
&B^{\text{hom}}_{21211} = D^{\text{hom}}_{21121} = -\frac{\mu}{2}\left(\frac{\left(5\alpha^2-1\right)}{\left(\alpha+1\right)^2}\right)\cdot L \\
&A^{\text{hom}}_{211211} = \frac{\mu}{24}\left(\frac{\left(79\alpha^4+16\alpha^3-6\alpha^2+16\alpha+7\right)}{\left(\alpha+1\right)^4}\right)\cdot L^2
\end{aligned}
\tag{41}
$$

We depict the dependence of the coupling and second gradient stiffness term of Eq. (41) in Fig. 3b.

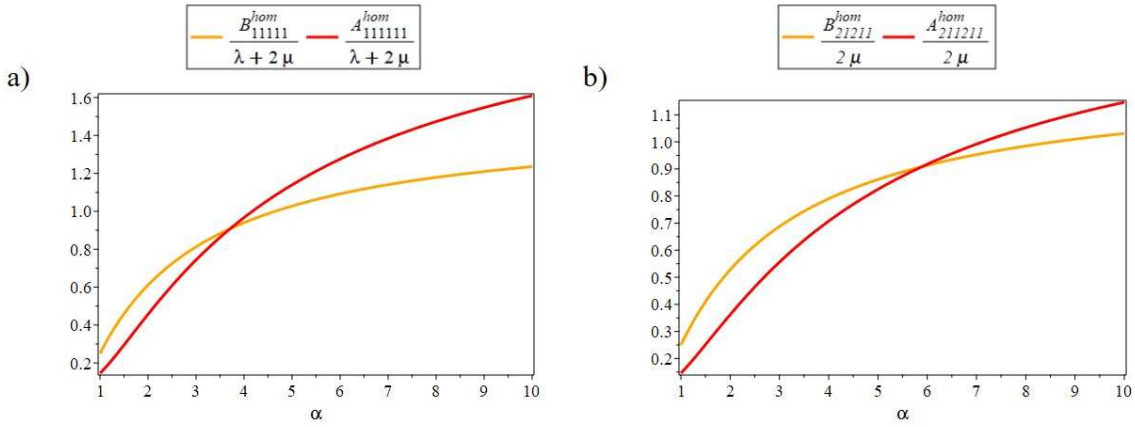

Figure 3: Homogenized second gradient and coupling tensors in function of layers thickness ratio d_1/d_2 for longitudinal (a) and for transverse (b)

Fig. 3 indicates that upon increasing geometric discrepancies of the layers within the unit-cell, the higher gradient contributions become more significant. We subsequently analyze the sensitivity of the second gradient terms on the moduli ratio value $\phi=E_2/E_1$ for the case of equal layer thickness $\left(d_1=d_2\right)$. We calculate the characteristic second gradient length $l_{e_{211}}$ to be:

$$
l_{e_{211}} = \sqrt{\frac{A^{\text{hom}}{}_{211211}}{C^{\text{hom}}{}_{2121}}} = 0.175\cdot L\sqrt{\frac{\phi(\phi+0.67)(\phi+0.49)(\phi+0.031)}{(\phi+0.67)^2\left(1.15\cdot 10^{-21}+0.0455\cdot\phi+0.0682\phi^2\right)}}
\tag{42}
$$

The characteristic length $l_{e_{211}}$ of Eq. (42) corresponding to equal layer thickness $(d_1 = d_2)$ is depicted in Fig. 4b as a function of ϕ along with the case where the thickness of the first layer is 1.5 times the thickness of the second layer.

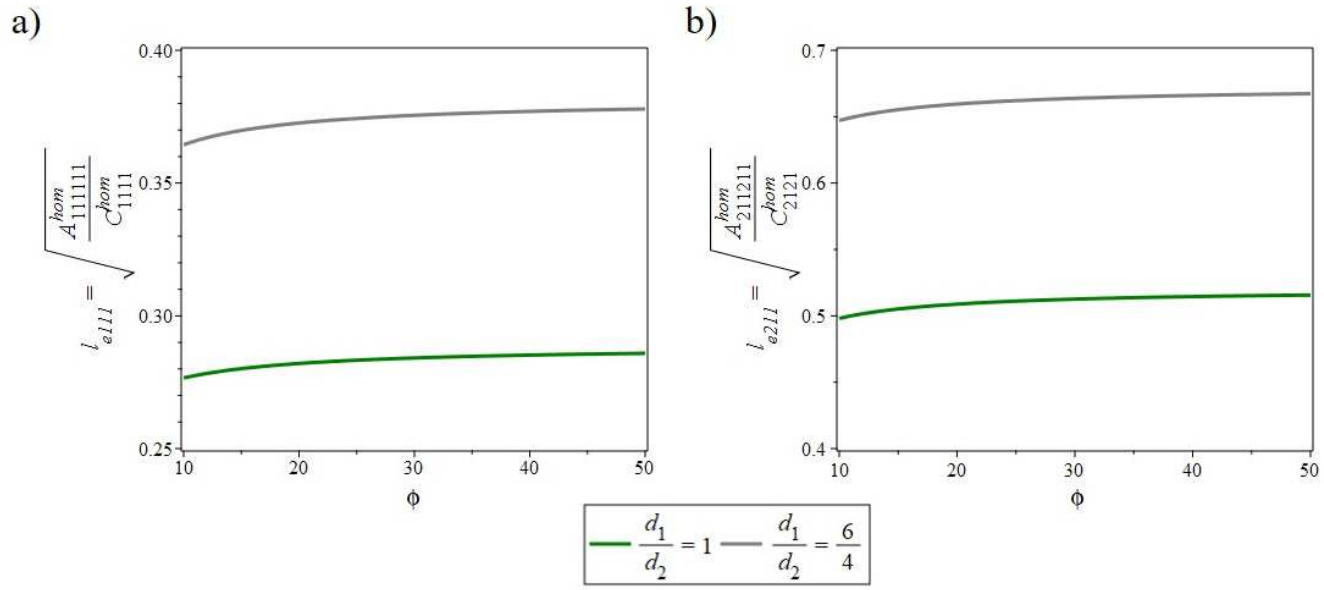

Figure 4: Second gradient characteristic length as a function of the elastic modulus ratio ϕ for the case of longitudinal and b) for transverse deformations (b) for different thickness ratio values.

Fig. (4b) suggests that as the contrast of the microscale material properties increases, the corresponding significance of second gradient effects increases for the transverse propagation mode. Thereupon, the first gradient is increasingly insufficient to describe the behavior of the medium as the inner contrast of the micro-scale material properties increases, whereas the second gradient significance increases.

3.3 Wave propagation in layered, periodic media

In the current section, we use the second gradient macroscopic dynamic equation of motion with micro-inertia effects to study the wave propagation characteristics of periodic, composite layered media. For the study, we use both the Hamilton formulation of Section 2.1.1 and the higher gradient energy method of Section 2.1.2 upon longitudinal and transverse deformations. We determine the dispersion characteristics of the propagating longitudinal and shear waves, as function of the propagating wave numbers (k). In particular, we compute the phase velocity (c), describing the

velocity at which the phase of any given frequency (w) travels within the medium and the group velocity (v_g), which describes the velocity of the envelope shape of the wave amplitudes. The phase and group velocity are defined as follows:

$$c = \frac{w}{k}, v_g = \frac{\partial w}{\partial k} \tag{43}$$

For the present study, we consider different material properties for each of the phases within the unit-cell structure of the periodic medium. The material properties of both phases are listed in Table 1.

Table 1: Geometric and mechanical layers properties

Properties	First layer	Second layer
Thickness	50%	50%
Poisson's ration	$\nu = 0.3$	$\nu = 0.3$
Shear modulus	$\mu_1 = 80760$ MPa	$\mu_2 = 8076$ MPa
Mass density	$\rho_1 = 8000$ Kg/m^3	$\rho_2 = 800$ Kg/m^3

For the computation of the wave propagation attributes, a harmonic wave propagation Ansatz is considered, with a displacement U_d being a function of the propagating wave numbers and frequency components, as follows:

$$U_d = U_0 e^{i\cdot\frac{\xi}{L}(X_1 - ct)} \tag{44}$$

In Eq. (44), U_0 stands for the displacement amplitude, k for the wave number and c for the phase velocity. The wave number is described in a normalized form $\xi = kL$, while i stands for the imaginary number, such that $i^2 = -1$. The subscript d is used to denote the direction of propagation, taking the values one for the longitudinal and two for the transverse.

3.3.1 Hamilton principle up to second gradient in dynamic state

In the current section, we use the second gradient Hamilton principle formulation of Section 2.2 to derive the macro equation of motion and the wave propagation characteristics of the laminated media, using the material properties in Table.1. To that purpose, we compute the homogenized first

order stress tensor $\left(\Sigma_{d1} = \frac{\partial W}{\partial E_{ij}} \right)$, using Eq. (18) for the longitudinal and transverse mode, along with the constants calculated in Eqs. (31,38). Thereupon, we obtain:

$$\Sigma_{d1} = U_0 \cdot \xi e^{-I(ct-X1)\xi} (\mathrm{H}_1^d \cdot \xi + \mathrm{H}_2^d \cdot I) \tag{45}$$

wherein the parameters H_1^d and H_2^d are constants summarized in Table 2. We compute accordingly the hyper-stress using Eq. (18) as the following expression:

$$S_{d1} = \frac{\partial W}{\partial K_{ijk}} = U_0 \xi e^{(-I(ct-X1)\xi)} (\mathrm{H}_3^d \cdot \xi + \mathrm{H}_4^d \cdot I) \tag{46}$$

wherein the parameters H_3^d and H_4^d are constants summarized in Table 2. Using Eq. (20), we calculate the homogenized macro-inertia forces on the laminated medium as follows:

$$\begin{aligned} F_d &= \frac{\partial}{\partial X_1}\left(\frac{1}{2}\ddot{E}_{d1} \left\langle \rho\left(H^E_{dd1} x_1 + H^E_{dd1} x_1 - 2x_1^2 \right) \right\rangle + \frac{1}{2}\ddot{K}_{d11} \left\langle \rho\left(H^K_{dd11} x_1 + \frac{1}{2} H^E_{dd1} x_1^2 - x_1^3 \right) \right\rangle \right) \\ &- \frac{\partial^2}{\partial X_1 \partial X_1}\left(\ddot{E}_{d1} \left\langle \frac{\rho}{2}\left(H^K_{dd11} x_1 + \frac{1}{2} H^E_{dd1} x_1^2 - x_1^3 \right) \right\rangle + \frac{1}{4}\ddot{K}_{d11} \left\langle \rho\left(H^K_{dd11} x_1^2 + H^K_{dd11} x_1^2 - x_1^4 \right) \right\rangle \right) \\ &= \frac{\partial}{\partial X_1}\left(\frac{1}{2}\ddot{E}_{d1} \left\langle \rho\left(H^E_{dd1} x_1 + H^E_{dd1} x_1 - 2x_1^2 \right) \right\rangle \right) - \frac{\partial^2}{\partial X_1 \partial X_1}\left(\frac{1}{4}\ddot{K}_{d11} \left\langle \rho\left(H^K_{dd11} x_1^2 + H^K_{dd11} x_1^2 - x_1^4 \right) \right\rangle \right) \\ &= \left(\mathrm{H}_5^d + \mathrm{H}_6^d \cdot \xi^2 \right) c^2 \xi^4 U_0 e^{(I\xi(-ct+X1))} \end{aligned} \tag{47}$$

where the parameters H_5^d and H_6^d in Eq. (47) are constants summarized in Table 2; we note that the coupling terms in the micro-inertia force cancel out. We substitute the expressions of the first, second order stress and micro inertia forces back into Eq. (17) and using the homogenized properties of the media (Eqs. (45-47)), we obtain the macro-equations of motion both for the longitudinal and the transverse mode, as follows:

$$\left(\mathrm{H}_1^d (H_7) + \mathrm{H}_4^d \right) \xi \cdot \mathrm{I} - \mathrm{H}_2^d (H_7) + \mathrm{H}_3^d \cdot \xi^2 + \mathrm{H}_5^d \cdot \xi^2 \mathrm{c}^2 (H_7)^3 + \mathrm{H}_6^d \cdot \xi^4 \mathrm{c}^2 (H_7)^3 - \rho^H \cdot \mathrm{c}^2 = 0 \tag{48}$$

Restricting the kinematics to the first gradient we obtain the following macro-equations of motion:

$$-\mathrm{H}_2^d (H_7) + \mathrm{H}_5^d \cdot \xi^2 \mathrm{c}^2 (H_7)^3 - \rho^H \cdot \mathrm{c}^2 = 0 \tag{49}$$

Equation of motion is Eq. (49) coincides with the one derived in [Wang and Sun, 2007]. The constants entering Eqs. (48) and (49) and used in subsequent computations are summarized in Table 2.

Table 2: Constant values obtained by the Hamilton principle based on second gradient mechanics

Mode constants	Longitudinal wave	Transverse wave
H_1^d	2336 MPa/m	1334 Mpa/m
H_2^d	51392.72 Mpa/m	29367.27 Mpa/m
H_3^d	-2238 Mpa	-1279 Mpa
H_4^d	-2336 Mpa	-1334 Mpa
H_5^d	122.72 kg/m^5	122.72 kg/m^5
H_6^d	13.7 kg/m^5	9.12 kg/m^5
H_7	1 m	1 m

We depict in Fig. 5 the dispersion characteristics of the laminated media using Eqs. (48) and (49) for the longitudinal mode in Fig. 5a and for the transverse mode in Fig. 5b. The second gradient Hamilton principle based results are shown with a cyan color, while the first gradient results in green. The latter have been already presented in (Wang and Sun, 2002). We further compare the results with the ones provided in (Bacigalupo and Gambarotta, 2014b) depicted in yellow, and with the exact solution of (Sun et al., 1968) in black. We make use of the periodicity of the medium along the X direction to obtain a better approximation of the dispersion curves, translating the wave vector for $k > \pi$ by 2π . The results in Fig. 5 are normalized with respect to the phase velocities at zero frequency for both modes, $\hat{c}_1 = 3.417 \cdot 10^3 m/s$ and $\hat{c}_2 = 2.58 \cdot 10^3$ m/s.

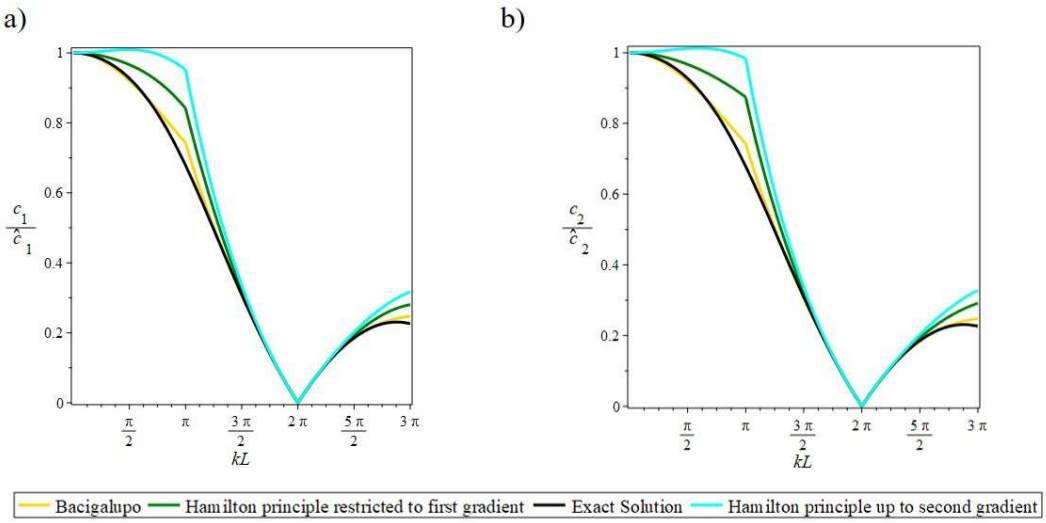

Figure 5: Phase velocity curves obtained by Hamilton principle up to second order (Cyan), for first gradient (green), first gradient with higher order micro-inertia effects (yellow) in (Bacigalupo & Gambarotta, 2014b) *and the exact solution (red) provided by* (Sun et al.,1968) *(Appendix C).*

The results of Fig. 5 show that the extension of Hamiltonian principle into second gradient doesn't provide an improvement with respect to first gradient results, yielding phase velocities which deviate from the exact solution to a greater extent than first order methods for wave number values close to $kL = \pi$. However, all methods converge to the exact solution predictions for higher wave number values.

In the next section, we develop the dynamic higher gradient energy homogenization method (DHGE) as an alternative approach for the computation of the effective behavior of the composite medium.

3.3.2 Higher gradient dynamic homogenization method

In the current section we use the DHGE method developed in Section 2.1.2 to study the wave propagation characteristics of laminated media upon both longitudinal and transverse deformations. Using the dynamic first and second gradient stress tensors evaluated in Section 2.1.2 (Eq. (22)) we compute the dispersion characteristics of the heterogeneous laminated medium when imposing a longitudinal harmonic wave normal to the layering. In this part we use the homogenized expressions of the dynamic tensors in function of the frequency, Eq. (24), for both longitudinal $(d=1)$ and transverse $(d=2)$ modes as follows:

$$
\begin{aligned}
C^{\hom,dyn}_{d1d1} &= \left\langle \frac{1}{2}\begin{pmatrix} A^E_{1dd1}C_{1dd1}A^E_{1dd1} + A^E_{d1d1}C_{d1d1}A^E_{d1d1} \\ +A^E_{1dd1}.C_{1dd1}.A^E_{d1d1} + A^E_{d1d1}.C_{d1d1}.A^E_{d1d1} \end{pmatrix} \right\rangle - w^2 \left\langle \frac{\rho}{2}\begin{pmatrix} H^E_{dd1}H^E_{dd1} + H^E_{dd1}H^E_{dd1} \\ -H^E_{dd1}x_1 - H^E_{dd1}x_1 \end{pmatrix} \right\rangle \\
&= C^d_1 - C^d_2 \cdot \xi^2 c^2 \\
B^{\hom,dyn}_{d1d11} &= \left\langle \frac{1}{2}\begin{pmatrix} A^E_{d1d1}C_{d1d1}A^K_{d1d11} + A^E_{1dd1}C_{1dd1}A^K_{d1d11} \\ +A^K_{d1d11}C_{d1d1}A^E_{d1d1} + A^K_{1dd11}C_{1dd1}A^E_{d1d1} \end{pmatrix} \right\rangle - w^2 \left\langle \frac{\rho}{2}\begin{pmatrix} H^K_{dd11}H^E_{dd1} + H^K_{dd11}H^E_{dd1} \\ -H^K_{dd11}x_1 - \frac{1}{2}H^E_{dd1}x_1x_1 \end{pmatrix} \right\rangle \\
&= C^d_3 - C^d_4 \cdot \xi^2 c^2 \\
D^{\hom,dyn}_{d11d1} &= \left\langle \begin{matrix} \frac{1}{2}\left(A^E_{d1d1}C_{d1d1}A^K_{d1d11} + A^E_{1dd1}C_{1dd1}A^K_{d1d11}\right) \\ +\frac{1}{2}\left(A^K_{d1d11}C_{d1d1}A^E_{d1d1} + A^E_{1dd1}C_{1dd1}A^K_{d1d11}\right) \end{matrix} \right\rangle - w^2 \left\langle \frac{\rho}{2}\begin{pmatrix} H^E_{dd1}H^K_{dd11} + H^E_{dd1}H^K_{dd11} \\ -\frac{1}{2}H^E_{dd1}x_1x_1 - H^K_{dd11}x_1 \end{pmatrix} \right\rangle \\
&= C^d_3 - C^d_4 \cdot \xi^2 c^2 \\
A^{\hom,dyn}_{d11d11} &= \left\langle \begin{matrix} \frac{1}{2}\left(A^K_{d1d11}C_{d1d1}A^K_{d1d11} + A^E_{1dd1}C_{1dd1}A^K_{d1d11}\right) \\ +\frac{1}{2}\left(A^K_{1dd11}C_{1dd1}A^K_{d1d11} + A^K_{d1d11}C_{d1d1}A^K_{d1d11}\right) \end{matrix} \right\rangle - w^2 \left\langle \frac{\rho}{2}\begin{pmatrix} H^K_{dd11}H^K_{dd11} + H^K_{dd11}H^K_{dd11} \\ -\frac{1}{2}H^K_{dd11}x_1x_1 - \frac{1}{2}H^K_{dd11}x_1x_1 \end{pmatrix} \right\rangle \\
&= C^d_5 - C^d_6 \cdot \xi^2 c^2
\end{aligned}
\tag{51}
$$

Remark: we checked that the dynamical second gradient moduli vanish for a homogeneous laminate.

The constants C^d_1 to C^d_6 entering Eq. (51) are summarized in Table 3 for the case of the material properties listed in Table 1. Using the expressions of Eq. (51), we compute the sensitivity of the second gradient characteristics lengths (l_{e111}, l_{e211}) as a function of the normalized wavenumber (kL) for different values of the phase velocity, for the case of longitudinal (Fig. 6a, $c_1/\hat{c}_1$) and transverse deformations (Fig. 6b, $c_2/\hat{c}_2$).

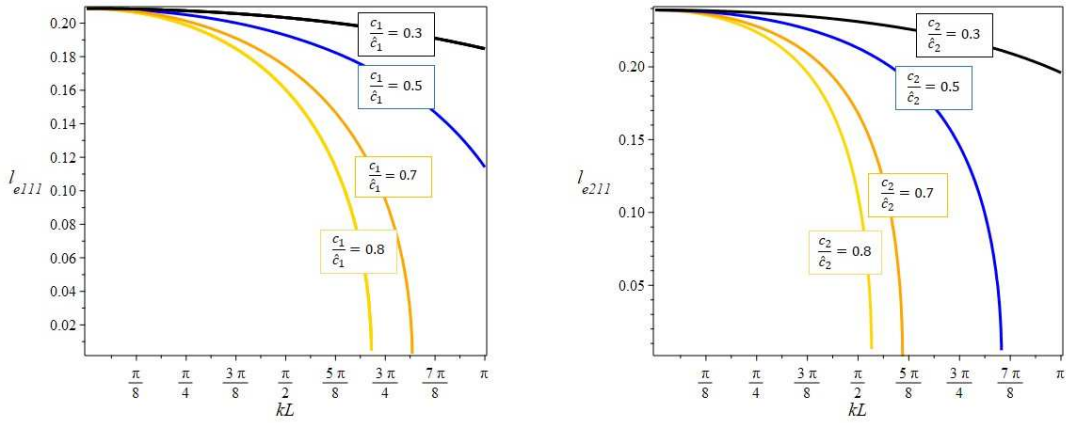

Figure 6: Variation of dynamic second gradient characteristic length as a function of the normalized wavenumber for different values of the phase velocity for the case of longitudinal (a) and transverse (b) deformation mode.

The tensors in Eq. (51) are used to calculate the homogenized stress and hyper-stress constitutive expressions of Eq. (7), presented in Eq. (52) with modified index notation:

$$\begin{aligned} \Sigma_{d1}^{dyn} &= C_{d1d1}^{\hom,dyn} E_{d1} + B_{d1d11}^{\hom,dyn} K_{d11} \\ S_{d11}^{dyn} &= D_{d1d11}^{\hom,dyn} E_{d1} + A_{d11d11}^{\hom,dyn} K_{d11} \end{aligned} \tag{52}$$

Using the homogenized constitutive expressions of Eq. (52), we write the equilibrium equation of motion as follows:

$$\nabla_{X_1} \left(\Sigma^{dyn}{}_{d1} - \nabla_{X_1} S^{dyn}{}_{d11} \right) = \rho \ddot{U}_d \tag{53}$$

Inserting Eq. (51) and Eq. (51) into Eq. (53) the wave equation of motion is retrieved to determine the dispersion relation of the wave in the two modes (longitudinal and transverse), as follows:

$$\frac{1}{d}\left((\mathrm{C}_1^d - \mathrm{C}_2^d \cdot \xi^2 \mathrm{c}^2)\xi^2 \cdot (\mathrm{C}_7)^3 + (\mathrm{C}_5^d - \mathrm{C}_6^d \cdot \xi^2 c^2)\xi^4 \mathrm{C}_7 \right) - \rho^{\hom} (C_7)^3 \xi^2 \mathrm{c}^2 = 0 \tag{54}$$

Restricting the kinematics to the first gradient weobtain the following macro-equation of motion:

$$\frac{1}{d}\left((\mathrm{C}_1^d - \mathrm{C}_2^d \cdot \xi^2 \mathrm{c}^2)\xi^2 \cdot (\mathrm{C}_7)^3 \right) - \rho^{\hom} (C_7)^3 \xi^2 \mathrm{c}^2 = 0 \tag{55}$$

All constants entering Eqs. (54) and (55) are summarized in Table 3.

Table 3: Constants value obtained by the DHGE method

Mode constants	Longitudinal mode	Transverse mode
C_1^d	51392.72 MPa	58734.54 MPa
C_2^d	$368.1\ kg/m^3$	$1227.27\ kg/m^3$
C_3^d	$-2336\ MPa \cdot m$	$-2669\ MPa \cdot m$
C_4^d	$-152\ kg/m^2$	$-289\ kg/m^2$
C_5^d	$2238\ MPa \cdot m^2$	$2558\ MPa \cdot m$
C_6^d	$59\ kg/m$	$78\ kg/m$
C_7	$1\ m$	$1\ m$
$\hat{c}_d$	$3.417 \cdot 10^3\ m/s$	$2.58 \cdot 10^3$ m/s

The first gradient wave equation restricts to the second power of the normalized wave vector $\left(\xi^2\right)$. We subsequently compare the second gradient homogenization results with the analytical solution provided by (Sun et al., 1968) and the results in (Bacigalupo & Gambarotta, 2014a). In Fig. 6, we plot the normalized phase velocity $\left(c_d / \hat{c}_d\right)$ where the phase velocities of the longitudinal mode $\hat{c}_1$ and of the shear mode $\hat{c}_2$ are calculated using the homogenized first gradient tensor of Eq. (24) in the static analysis case $\left(\hat{c}_d = \sqrt{C^{\hom,Static}_{d1d1} / \rho^{\hom}}, w = 0\right)$, using material properties summarized in Table 1. The phase velocity computed by the DHGE method (Eq. (54, 55)) is depicted in red, while a blue dashed line is used for the first gradient computations. The asymptotic homogenization results are depicted in yellow and the exact solution (**Appendix C**) in black. Fig.6a provides the longitudinal mode results, while Fig. 6b the ones corresponding to the transverse mode.

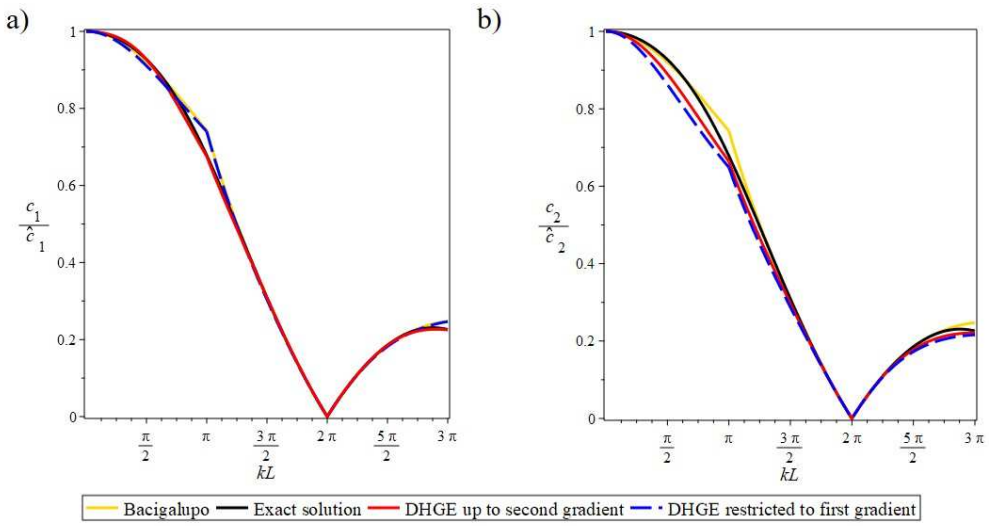

Figure 7: Normalized phase velocity curves for longitudinal wave (a) and for transverse wave (b) obtained by the DHGE method with first and second gradient constitutive parameters (blue and red respectively). The exact solution is presented in black (Sun et al., 1968), while the yellow color curves correspond to the first gradient constitutive formulation with higher gradient inner micro-inertia terms provided in (Bacigalupo & Gambarotta, 2014)

Fig. 7 indicates that the DHGE method provides a very good agreement with the exact solution (black) over the entire range of normalized wave number values both for the longitudinal and for the transverse mode. The first gradient results (blue) are very close to the first gradient constitutive modeling results with higher gradient micro-inertia terms (yellow curves) in the left plot of Fig. 7a

We subsequently compute the normalized frequency w / w_0 in Fig. 8a,b, the normalization being carried out with respect to the natural frequency, defined as $w_0 = \hat{c}_d / L$ which is equal to the wave velocity since we deal with a laminated cell of unit length; the normalized frequency together with the group velocity (Fig. 8c,d) are recorded versus the wavenumber.

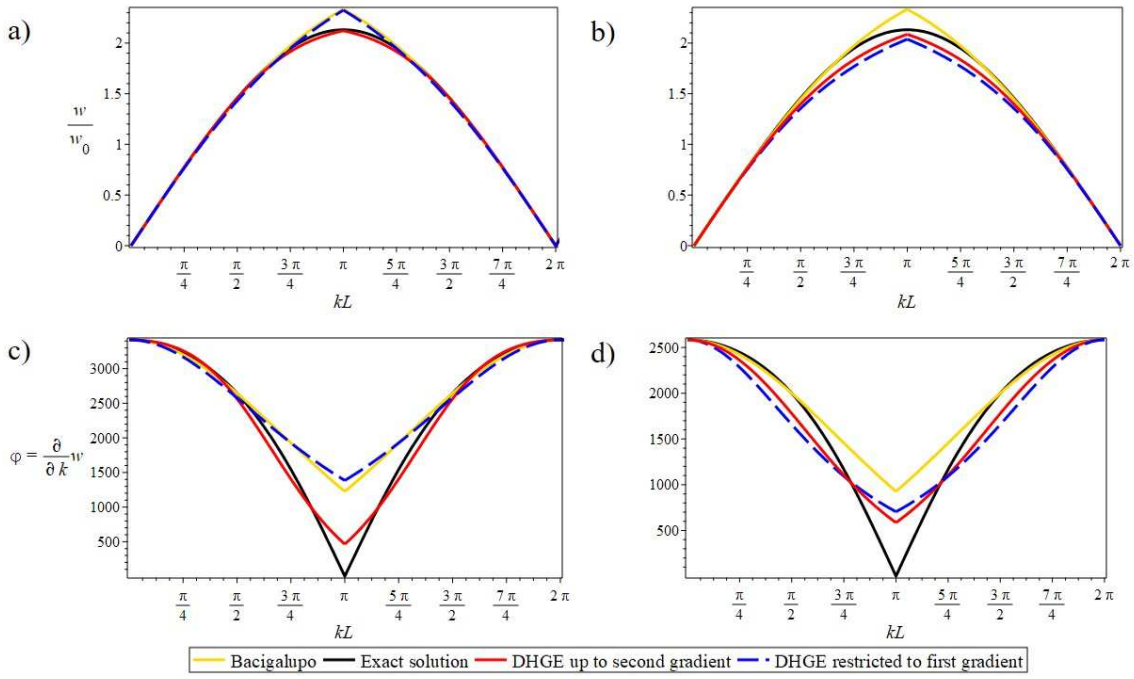

Figure 8: Frequency of the longitudinal (a) and transverse waves (b) and group velocity for the longitudinal (c) and transverse waves (d) for both dynamic homogenization methods as a function of the propagating wave number value

Figures 8a and 8b indicate that the exact solution predicts a maximum frequency value for a propagating wave number $kL = \pi$, with a continuous frequency gradient, so that $w'(\pi^-) = w'(\pi^+)$. The near zero slope applies for the second gradient homogenization method of Section 2.1.2, while all other approaches lead to a more prominent discontinuity point for a normalized wavenumber value of $kL = \pi$. The continuous frequency plots at $kL = \pi$ require a zero group velocity at the same point, as indicated by the black curves of Fig. 8c and 8d. The dynamic, second gradient constitutive formulation is closer to the minimum group velocity for both the longitudinal and the transverse mode, with first gradient formulations to predict notably higher values (Figs. 8c, 8d).

4. Discussion

The results of Section 3 suggest that the significance of higher gradient constitutive terms in the presence of micro-inertia effects depends both on the geometric and on the material properties of the underlying microstructure. In particular, the coupling and second gradient terms increase upon increasing difference of the relative fraction (d_1/d_2) of the phases contained within the unit-cell architecture, as shown in Fig. 3. What is more, the evolution of the second gradient characteristic lengths indicate that higher order effects become more prominent upon increasing differences in the moduli of the phases contained within the unit cell (ϕ) for the longitudinal mode (Fig. 4a) and for the transverse mode (Fig. 4b), with the most prominent changes to take place upon geometric rather than material differences in the underlying microstructural phases.

The second gradient effects depend, not only on the geometric and material parameters of the underlying unit-cell architecture, but also on the propagating wave-number of interest. This can be observed in Fig. 7, where the addition of second gradient effects improves the consistency of the computed results (red curve in Fig. 7a) for wavenumbers close to $kL=\pi$ with respect to the Floquet-Bloch, elasticity-based solution. The differences observed for moderate wavenumbers vanish in the higher wavenumber regime of $kL=2\pi$, where all formulations yield the same predictions with the one provided by the elasticity solution (**Appendix C**).

The higher gradient constitutive modelling results are considerably sensitive to the formulation used for their derivation. In particular, using the Hamilton's principle which involves the static Cauchy and hyperstress tensors (the second gradient formulation in Section 3.2.1) leads to phase velocity predictions which substantially differ from the ones predicted by the elasticity-based, Floquet-Bloch results or from first gradient constitutive modelling approximations in the wavenumber region close to $kL=\pi$, both for the longitudinal (Fig. 5a) and for the transverse mode (Fig. 5b). The recorded differences can be primarily attributed to the fact that the dynamic, micro-inertia terms of Eq. (5) contribute solely to the potential energy part P' and not to the kinetic energy part T' of Eq. (11), in which only higher strain gradient terms appear (Eqs. (11)-(13)). The overestimation of the phase velocity for Hamilton-based methods in the wavenumber region $kL=\pi$ is already visible for first gradient constitutive modeling results (green curves in Fig. 5), an observation made in previous contributions (Wang and Sun 2002, Sun and Huang 2007). In this wavenumber space and upon the Hamilton formulation, the Floquet-Bloch results are best approximated by higher asymptotic expansion contributions of the micro-inertia terms with the macroscopic constitutive parameters retained to their first-order approximation (Bacigalupo &

Gambarotta, 2014b). However, the dispersion curves retain a discontinuous rate of change at $kL=\pi$, contrary to the continuous elasticity theory predictions.

The dynamic, second gradient constitutive modeling results obtained based on the Hamilton's principle in Section 3.2.1, fundamentally differ from the ones obtained with the use of the dynamic higher gradient energy method of Section 3.2.2, for which the Hill-Mandel expression is directly used to compute the total internal energy stored in the medium (Section 2.1.2). Thereupon, the derived macro-stress and hyperstress are frequency dependent (Section 2.1.2) and not static as in the Hamilton principle based derivations (Section 2.1.1). In the energy based method, the micro-inertia effects related to each of the constitutive tensors can be directly assessed, contrary to the Hamilton formulation, where the constitutive terms are static and not dynamic, with the micro-inertia effects to be assimilated in the F_i term of Eq. (19).

The DHGE method yields high consistency results throughout the entire wavenumber range, as it can be observed from the dispersion curves of Fig. 7 and from the frequency and group velocity curves of Fig. 8. More specifically, first order gradient based methods lead to an inflection point at $kL=\pi$ (Fig. 7), a discontinuity which is not present for the Floquet-Bloch solution or nearly disappears for the higher gradient based homogenization method results in Fig. 7 (red). For normalized wavenumbers equal to $kL=\pi$, the frequency does not depend on position – as the Floquet-Bloch results suggest -, so that a transition from planar to standing waves takes place (frequency depends only on time and not on position). This is expressed in the frequency plots of Fig. 8a and 8b, where the first gradient constitutive results (yellow and blue curves) do not provide continuous frequencies, while their corresponding group velocities are far from zero. Contrariwise, the second gradient formulation elaborated in Section 3.2.2 yields a nearly continuous frequency curve slope, with a group velocity value that approaches zero at the maximum frequency point (Fig. 8c, 8d).

5. Conclusion

Overall, in the current work, a dynamic higher gradient constitutive model with micro-inertia effects has been developed for the computation of the static and dynamic attributes of heterogeneous materials with an inner microstructure. The method has been used to compute the macroscopic static and dynamic second gradient constitutive parameters of two-phase composite layered materials, using both the Hamilton's principle and the total internal higher gradient energy. The sensitivity of the second gradient constitutive parameters has been analyzed as a function of the inner material and geometric microstructural parameters for the case of layered two-phase composite structure. It has

been noted that the significance of second gradient terms increases, upon increasing differences in the volumetric ratio and in the material properties of the microstructural phases for both longitudinal and transverse deformation patterns. What is more, evidence has been provided that the incorporation of higher gradient macroscopic constitutive parameters can well describe the wave propagation characteristics of the micro-structured media when formulated using the Hill-Mandel equality in the context of its total, dynamic higher gradient deformation energy. The latter yields high accuracy results for the propagating phase and group velocities over the entire wave-number space, outperforming first order constitutive formulations.

6. References

Aifantis, E., (1992). International Journal of Engineering Science 30(10):1279-1299. doi: 10.1016/0020-7225(92)90141-3.

Aifantis, E., (1998). Strain gradient interpretation of size effects. International Journal of Fracture, 95(1), 299-314.doi: 10.1023/A:1018625006804.

Alibert, J.J., Della Corte, A., (2015). Second-gradient continua as homogenized limit of pantographic microstructured plates: a rigorous proof. Zeitschrift für angewandte Mathematik und Physik. 66(5), 2855-2870.

Andrianov, I.V., Bolshakov, V.I., Danishevs'kyy, V.V., Weichert, D., (2008). Higher order asymptotic homogenization and wave propagation in periodic composite materials. Proceedings of the Royal Society A, 464(2093), 1181–1201. https://doi.org/10.1098/rspa.2007.0267.

Andrianov, I.V., Awrejcewicz, J., Danishevs'kyy, V.V., Weichert, D., (2011). Wave propagation in periodic composites: higher-order asymptotic analysis versus plane-wave expansion method. Journal of Computational and Nonlinear Dynamics 6(1), 011015-1 - 011015-8.DOI: 10.1115/1.4002389.

Andrianov, I., Awrejcewicz, J., Weichert, D., (2010). Improved Continuous Models for Discrete Media. Mathematical Problems in Engineering, http://dx.doi.org/10.1155/2010/986242.

Auriault, J.L., Boutin, C., (2012). Long wavelength inner-resonance cut-off frequencies in elastic composite materials. International Journal of Solids and Structures, 49(23–24), 3269-3281.

Askes, H., Aifantis, E., (2009). Gradient elasticity and flexural wave dispersion in carbon nanotubes. Phys. Rev. B 80, 195412.

Askes, H., Aifantis, E., (2011). Gradient elasticity in statics and dynamics: An overview of formulations, length scale identification procedures, finite element implementations and new results. International Journal of Solids and Structures,48(13),1962-1990.

Askes, H., Calik-Carakose, U., Susmel, L., (2012). Gradient elasticity length scale validation using static fracture experiments of PMMA and PVC. International Journal of Fracture, 176(2), 223–227. doi:10.1007/s10704-012-9735-x.

Askes, H., Metrikine, A., (2002). One-dimensional dynamically consistent gradient elasticity models derived from a discrete microstructure: Part 2: Static and dynamic response. European Journal of Mechanics - A/Solids, 21(4), 573-588. doi.org/10.1016/S0997-7538(02)01217-2.

Askes, H., Metrikine, A., Pichugin, A., Bennett, T., (2008). Four simplified gradient elasticity models forvthe simulation of dispersive wave propagation. Journal Philosophical Magazine , 88(28-29) 3415-3443. doi.org/10.1080/14786430802524108.

Bacigalupo, A., Gambarotta, L., 2010. Strain-gradient computational homogenization of heterogeneous materials with periodic microstructure. ZAMM Z. Angew. Math. Mech. 90, 796–811. https://doi.org/10.1016/j.ijsolstr.2012.07.002.

Bacigalupo, A., Gambarotta, L., (2012). Computational two-scale homogenization of periodic masonry: characteristic lengths and dispersive waves. Computer Methods in Applied Mechanics and Engineering, 213–216, 16-28. doi.org/10.1016/j.cma.2011.11.020.

Bacigalupo, A. (2014a). Second-order homogenization of periodic materials based on asymptotic approximation of the strain energy: formulation and validity limits. Materials Science (cond-mat.mtrl-sci). arXiv:1401.7855.

Bacigalupo, A., Gambarotta, L., (2014b). Second-gradient homogenized model for wave propagation in heterogeneous periodic media. International Journal of Solids and Structures, 51(5) 1052-1065.https://doi.org/10.1016/j.ijsolstr.2013.12.001.

Bakhvalov, N.S., Panasenko, G.P., (1984). Homogenization, Averaging process in periodic Media. Kluwer Academic Publishers. Moscow.

Bensoussan, A., Lions, J.L., Papanicolaou, G., (1978). Asymptotic Analysis for periodic structures. Amsterdam, New York, North-Holland Pub. www.ams.org/bookpages/chel-374.

Berezovski, A., Engelbrecht, J., Salupere, A., Tamm, K., Peets, T., Berezovski, M., (2013). Dispersive waves in microstructured solids. International Journal of Solids and Structures, 50(11–12) 1981-1990.doi: https://doi.org/10.1016/j.ijsolstr.2013.02.018.

Boutin, C., Auriault, J.L., (1993). Rayleigh scattering in elastic composite materials. International Journal of Engineering Science, 31(12) 1669-1689. https://doi.org/10.1016/0020-7225(93)90082-6.

Claude Boutin, (1996). Microstructural effects in elastic composites. International Journal of Solids and Structures, 33 (7) 1023-105.

Chen, W., Fish, J., (2000). A dispersive model for wave propagation in periodic heterogeneous media based on homogenization with multiple spatial and temporal scales. Journal of Applied Mechanics, 68(2), 153-161. doi:10.1115/1.1357165.

Craster, R.V., Kaplunov, J., Pichugin, A.V., (2010). High-frequency homogenization for periodic media. Proceedings of the Royal Society A, 466, 2341–2362. https://doi.org/10.1098/rspa.2009.0612.

Erofeyev, V. I., (2003). Wave Processes in Solids with Microstructure. World Scientific, 2003.

Fafalis, D., Filopoulos, S., Tsamasphyros, G., (2012). On the capability of generalized continuum theories to capture dispersion characteristics at the atomic scale. European Journal of Mechanics - A/Solids, 36, 25–37. doi:10.1016/j.euromechsol.2012.02.004.

Fish, J., Chen., (2001). W, Higher-order homogenization of initial/boundary-value problem, J. Eng. Mech. 127, 1223-1230.

Gonella, S., Steven Greene, M., & Liu, W. K. (2011). Characterization of heterogeneous solids via wave methods in computational microelasticity. Journal of the Mechanics and Physics of Solids, 59(5), 959-974. https://doi.org/10.1016/j.jmps.2011.03.003.

Gonella, S., Ruzzene, M., (2010). Multicell homogenization of one-dimensional periodic structures. Journal of Vibration and Acoustics, 132(1). https://doi:10.1115/1.4000439.

Gourgiotis, P., Georgiadis, H., (2009). Plane-strain crack problems in microstructured solids governed by dipolar gradient elasticity. Journal of the Mechanics and Physics of Solids 57(11) 1898-1920. Doi: 10.1016/j.jmps.2009.07.005.

Guenneau, S., Craster, R., Antonakakis, T., Cherednichenko, K., Cooper, S., (2013). Homogenization Techniques for Periodic Structures. E. Popov. Gratings: Theory and Numeric Applications, AMU (PUP), pp.11.1-11.31. https://hal.archives-ouvertes.fr/hal-00785718.

Gutkin, M., Aifantis, E., (1999). Dislocations in the theory of gradient elasticity. Scripta Mater 40, 559-566.

Huang, Z.G., 2011. Analysis of Acoustic Wave in Homogeneous and Inhomogeneous Media Using Finite Element Method. Acoustic Waves - From Microdevices to Helioseismology, Marco G. Beghi, IntechOpen.DOI: 10.5772/18792.

Hussein, M.I., (2009). Reduced Bloch mode expansion for periodic media band structure calculations. Proceedings of the Royal Society A, 465, 2825–2848. https://doi.org/10.1098/rspa.2008.0471.

Iliopoulos, S., Aggelis,D., Polyzos, D., (2016). Wave dispersion in fresh and hardened concrete through the prism of gradient elasticity, International Journal of Solids and Structures, 78–79, 149-159. https://doi.org/10.1016/j.ijsolstr.2015.09.005.

Karathanasopoulos, N., Reda, H., & Ganghoffer, J. F. (2019). The role of non-slender inner structural designs on the linear and non-linear wave propagation attributes of periodic, two-dimensional architectured materials. Journal of Sound and Vibration, 455, 312–323. https://doi.org/10.1016/J.JSV.2019.05.011.

Koiter,W.T., (1969). Couple-stresses in the theory of elasticity: I and II. Philosophical transactions of the royal society of London OF LONDON B, 67 ,17-44.

Lombardo, M., Askes, H., (2012). Higher-order gradient continuum modelling of periodic lattice materials. Computational Materials Science, 52(1), 204-208. https://doi.org/10.1016/j.commatsci.2011.05.025.

Metrikine, A.V., Askes, H., (2002). One-dimensional dynamically consistent gradient elasticity models derived from a discrete microstructure: Part 1: Generic formulation. European Journal of Mechanics - A/Solids 21(4), 555-572. DOI: 10.1016/S0997-7538(02)01218-4.

Mindlin, R.D., (1964). Micro-structure in linear elasticity. Archive for Rational Mechanics and Analysis, 16(1), 51–78. https://doi.org/10.1007/BF00248490.

Mindlin, R., (1965). Second gradient of strain and surface-tension in linear elasticity. International Journal of Solids and Structures, 1(4), 417-438. https://doi.org/10.1016/0020-7683(65)90006-5.

Mindlin, R.D., (1972). Elasticity, piezoelectricity and crystal lattice dynamics. Journal of Elasticity, 2(4), 217–282. https://doi.org/10.1007/BF00045712.

Muhlhaus, H., Oka, F., (1996). Dispersion and wave propagation in discrete and continuous models for granular materials. International Journal of Solids and Structures, 33(19), 2841-2858. Doi: 10.1016/0020-7683(95)00178-6.

Nemat-Nasser, S., Srivastava, A., (2011). Overall dynamic constitutive relations of layered elastic composites. Journal of the Mechanics and Physics of Solids 59(10),1953-1965.Doi: 10.1016/j.jmps.2011.07.008.

Nemat-Nasser, S., Srivastava, A., (2012). Overall dynamic properties of three-dimensional periodic elastic composites. Proceedings of the Royal Society A Mathematical Physical and Engineering Sciences, 468(2137), 269-287. Doi: 10.1098/rspa.2011.0440.

Ostoja-Starzewki, M., (2002). Lattice models in micromechanics. Applied Mechanics Reviews, 55(1), 35-60.doi:10.1115/1.1432990.

Papargyri-Beskou, S., Polyzos, D., Beskos. D.E., (2009). Wave dispersion in gradient elastic solids and structures: a unified treatment. International Journal of Solids and Structures 46 (21), 3751-3759. https://doi.org/10.1016/j.ijsolstr.2009.05.002.

Papargyri-Beskou, S., Beskos, D.E., (2004). Response of gradient-viscoelastic bar to static and dynamic axial load. Acta Mechanica, 170(3–4), 199–212. https://doi.org/10.1007/s00707-004-0106-1.

Polyzos, D., Huber, G., Mylonakis, G., Triantafyllidis, T., Papargyri-Beskou, S., Beskos, D.E., (2015). Torsional vibrations of a column of fine-grained material: A gradient elastic approach. Journal of the Mechanics and Physics of Solids, 76, 338-358. https://doi.org/10.1016/j.jmps.2014.11.012.

Reda, H., Karathanasopoulos, N., Rahali, Y., Ganghoffer, J. F., & Lakiss, H. (2018a). Influence of first to second gradient coupling energy terms on the wave propagation of three-dimensional non-centrosymmetric architectured materials. International Journal of Engineering Science, 128, 151–164. https://doi.org/10.1016/J.IJENGSCI.2018.03.014.

Reda, H., Karathanasopoulos, N., Ganghoffer, J. F., & Lakiss, H. (2018b). Wave propagation characteristics of periodic structures accounting for the effect of their higher order inner material kinematics. Journal of Sound and Vibration, 431, 265–275. https://doi.org/10.1016/J.JSV.2018.06.006

Reda, H., Karathanasopoulos, N., Elnady K., Ganghoffer, J. F., & Lakiss, H. (2018c), The role of anisotropy on the static and wave propagation characteristics of two-dimensional architectured materials under finite strains, Materials and design, 147, 134-145, 2018, https://doi.org/10.1016/j.matdes.2018.03.039

Réthoré, J., Kaltenbrunner, C., Dang, T., Chaudet, P., Kuhn, M., (2015). Gradient-elasticity for honeycomb materials: Validation and identification from full-field measurements. International Journal of Solids and Structures, 72, 108-117. https://doi.org/10.1016/j.ijsolstr.2015.07.015.

Robinson, C. W., Leppelmeier, G. W., (1974). Experimental Verification of Dispersion Relations for Layered Composites. Journal of Applied Mechanics, 41(1). Doi: 10.1115/1.3423280.

Sanchez Palencia, E., (1980). Non-Homogeneous Media and Vibration Theory. Lecture Notes in Physics, 127, Springer, Berlin.

Smyshlyaev, V.P., Cherednichenko, K.D.,(2000). On rigorous derivation of strain gradient effects in the overall behaviour of periodic heterogeneous media. Journal of the Mechanics and Physics of Solids 48(6):1325-1357. DOI: 10.1016/S0022-5096(99)00090-3.

Smyshlyaev, V.P., (2009). Propagation and localization of elastic waves in highly anisotropic periodic composites via two-scale homogenization. Mechanics of Materials, 41(4), 434-447. https://doi.org/10.1016/j.mechmat.2009.01.009.

Sun, C.T., Achenbach, J.D., Herrmann, G., (1968). Time-harmonic waves in a stratified medium propagating in the direction of the layering. Journal of Applied Mechanics, 35(2), 408-411. doi:10.1115/1.3601212.

Sun, C.T., Huang, G.L., (2006). Modeling Heterogeneous Media with Microstructures of Different Scales. Journal of Applied Mechanics, 74(2), 203–209. doi:10.1115/1.2188536.

Toupin, R.A., (1962). Elastic materials with couple-stresses. Archive for Rational Mechanics and Analysis, 11(1), 385–414. https://doi.org/10.1007/BF00253945.

Trinh, D.K., (2011). Méthodes d'homogénéisation d'ordre supérieur pour les matériaux architecturés. École nationale supérieure des Mines de Paris.

Trinh D.K., Janicke R., Auffray N., (2012). Evaluation of generalized continuum substitution models for heterogeneous materials. Journal for Multiscale Computational Engineering, 10 (6): 527–549. DOI: 10.1615/IntJMultCompEng.2012003105.

Vivar-Perez, J.M., Gabbert, U., Berger, H., Rodriguez-Ramos, R.,Bravo-Castillero, J., Guinovart-Diaz, R., Sabina, F.J., (2009). A dispersive nonlocal model for wave propagation in periodic composites. European Journal of Mechanics - A/Solids 82(3). DOI: 10.1016/j.euromechsol.2014.05.009.

Wang, Z.-P., Sun, C.T., (2002). Modelling micro-inertia in heterogeneous materials under dynamic loading. Wave Motion, 36(4), 473–485. DOI: 10.1016/S0165-2125(02)00037-9.

Zhikov, V.V., (2000). On an extension of the method of two-scale convergence and its applications. Sbornik: Mathematics, 191(7), 973-1014. DOI:10.1070/SM2000v191n07ABEH000491.

Appendix A: Hamilton principle

A.1 Second gradient from surface to volume integration

To derive the energy equation which link the macro-energy with the micro-energy and displacement we start by the following integral:

$$\int_{d\Omega}\left(u_i - x_j E_{ij} - \frac{1}{2}K_{ijk}x_j x_k\right)\left(\sigma_{mi} - \Sigma_{mi}\right).n_m ds \tag{A.1}$$

Using the divergence theorem we get the new form of this integral which is equal to zero (using the assumption of displacement on the boundaries):

$$\int_{\Omega}\left(\varepsilon_{im} - \delta_{jm}E_{ij} - \frac{1}{2}K_{ijk}\delta_{jm}x_k - \frac{1}{2}K_{ijk}\delta_{km}x_j\right).\left(\sigma_{mi} - \Sigma_{mi}\right) +$$
$$\left(u_i - x_j E_{ij} - \frac{1}{2}K_{ijk}x_j x_k\right)\left(\sigma_{mi,m}\right)d\Omega$$

$$0 = \left\langle \varepsilon_{im}\sigma_{mi}\right\rangle - E_{im}\Sigma_{mi} - \frac{1}{2}K_{imk}\left\langle x_k\sigma_{mi}\right\rangle - \frac{1}{2}K_{ijm}\left\langle x_j\sigma_{mi}\right\rangle + \frac{1}{2}K_{imk}\left\langle x_k\right\rangle\Sigma_{mi} + \frac{1}{2}K_{ijm}\left\langle x_j\right\rangle.\Sigma_{mi}$$
$$+\left\langle u_i\rho\ddot{u}_i\right\rangle - E_{ij}\left\langle x_j\rho\ddot{u}_i\right\rangle - \frac{1}{2}K_{ijk}\left\langle x_j x_k\rho\ddot{u}_i\right\rangle \tag{A.2}$$

$$\Rightarrow E_{ik}\Sigma_{ki} = \left\langle \varepsilon_{ik}\sigma_{ki}\right\rangle - \frac{1}{2}K_{ijk}\left\langle x_k\sigma_{ji}\right\rangle - \frac{1}{2}K_{ijk}\left\langle x_j\sigma_{ki}\right\rangle + \left\langle u_i\rho\ddot{u}_i\right\rangle - E_{ij}\left\langle \rho\ddot{u}_i x_j\right\rangle - \frac{1}{2}K_{ijk}\left\langle x_j x_k\rho\ddot{u}_i\right\rangle$$

$$\Rightarrow E_{ij}\Sigma_{ij} = \left\langle \varepsilon_{ij}\sigma_{ij}\right\rangle - K_{ijk}S_{ijk} + \left\langle u_i\rho\ddot{u}_i\right\rangle - E_{ij}\left\langle \rho\ddot{u}_i x_j\right\rangle - \frac{1}{2}K_{ijk}\left\langle x_j x_k\rho\ddot{u}_i\right\rangle$$

$$\Rightarrow E_{ij}\Sigma_{ij} + K_{ijk}S_{ijk} = \left\langle \varepsilon_{ij}\sigma_{ij}\right\rangle + \left\langle \rho\ddot{u}_i\left(u_i - E_{ij}x_j - \frac{1}{2}K_{ijk}x_j x_k\right)\right\rangle$$

A.2 Hamiltonian principle up to second gradient

$$\delta \int_{V,t} \left(\frac{1}{2} \langle \rho \rangle \dot{U}_i \dot{U}_i + T' - \left(\frac{1}{2} E_{ij} \Sigma_{ij} + \frac{1}{2} K_{ijk} S_{ijk} + P' \right) \right) dVdt = 0 \tag{A.3}$$

We start to calculate using the integration by parts of each integral:

$$Integral_1 = \delta \int_{V,t} \left(\frac{1}{2} E_{ij} \Sigma_{ij} \right) dVdt \tag{A.4}$$

We note that that the effective stress can be defined from the strain energy density $w(E)$:

$$\begin{aligned} &\Sigma_{ij} = \frac{\partial w(E,K)}{\partial E_{ij}} \\ &\delta \int w dVdt = \int \delta w dVdt = \int \frac{\partial w}{\partial E_{ij}} \partial E_{ij} dVdt = \int \Sigma_{ij} \delta E_{ij} dVdt = \int \Sigma_{ij} \delta \left(\frac{U_{i,j} + U_{j,i}}{2} \right) dVdt = \int \Sigma_{ij} \delta U_{i,j} dVdt \\ &\Rightarrow Integral_1 = \delta \int \frac{1}{2} E_{ij} \Sigma_{ij} dVdt = \int \Sigma_{ij} \delta U_{i,j} dVdt = \int \Sigma_{ij} \delta U_i n_j dVdt - \int \Sigma_{ij,j} \delta U_i dVdt \\ &= S_1 - \int \Sigma_{ij,j} \delta U_i dVdt \end{aligned} \tag{A.5}$$

Similarly, the hyperstress tensor derives from the same strain energy density as:

$$S_{ijk} = \frac{\partial w(E,K)}{\partial K_{ijk}} \tag{A.6}$$

Then, it holds due to Euler theorem for functions homogeneous of degree two:

$$K_{ijk} \frac{\partial Z}{\partial K_{ijk}} = 2Z \Rightarrow Z = \frac{1}{2} K_{ijk} S_{ijk} \tag{A.7}$$

This entails the following variation (we note that in the following variation we will neglect the time constant because we will derive the final equation with respect to t):

$$
\begin{aligned}
&Integral_2 = \delta\int wdVdt = \int \delta w dVdt = \int \frac{\partial w}{\partial K_{ijk}}\delta K_{ijk} dVdt = \int S_{ijk}\delta K_{ijk} dVdt = \int S_{ijk}\delta U_{i,jk} dVdt \\
&= \delta\int S_{ijk}K_{ijk} dVdt = \int \left(S_{ijk}\delta U_{i,j}\right)_{,k} dVdt - \int S_{ijk,k}\delta U_{i,j} dVdt \\
&= \int \left(S_{ijk}\delta U_{i,j}\right) n_k dSdt - \int S_{ijk,k}\delta U_{i,j} dVdt \\
&= S_{2a} - \int S_{ijk,k}\delta U_{i,j} dVdt = S_{2a} - \left(\int \left(S_{ijk,k}\delta U_i\right)_{,j} dVdt - \int S_{ijk,kj}\delta U_i dVdt\right) \\
&= S_{2a} - \int \left(S_{ijk,k}\delta U_i\right)_{,j} dVdt + \int S_{ijk,kj}\delta U_i dVdt \\
&= S_{2a} - \int \left(S_{ijk,k}\delta U_i\right) n_j dSdt + \int S_{ijk,kj}\delta U_i dVdt = S_{2a} + S_{2b} + \int S_{ijk,kj}\delta U_i dVdt
\end{aligned}
\tag{A.8}
$$

$$
\begin{aligned}
&Integral_3 = \frac{1}{2}\int \delta\langle\rho\rangle \dot{U}_i \dot{U}_i dVdt = \int \langle\rho\rangle \delta\dot{U}_i \dot{U}_i dVdt \\
&= \langle\rho\rangle \delta U_i \dot{U}_i\Big|_{\Delta T} - \int \langle\rho\rangle \delta U_i \ddot{U}_i dVdt = S_3 - \int \langle\rho\rangle \delta U_i \ddot{U}_i dVdt
\end{aligned}
\tag{A.9}
$$

We next calculate the variation of the internal energy fluctuation:

$$
\begin{aligned}
&Integral_4 = \delta\int P'(E_{ij}, \ddot{E}_{ij}, K_{ijk}, \ddot{K}_{ijk}) dVdt = \int \frac{\partial P'}{\partial E_{ij}}\delta E_{ij} + \frac{\partial P'}{\partial \ddot{E}_{ij}}\delta\ddot{E}_{ij} + \frac{\partial P'}{\partial K_{ijk}}\delta\nabla E_{ij} + \frac{\partial P'}{\partial \ddot{K}_{ijk}}\delta\nabla\ddot{E}_{ij} dVdt \\
&= \int \frac{\partial P'}{\partial E_{ij}}\delta E_{ij} + \frac{\partial P'}{\partial \ddot{E}_{ij}}\delta\ddot{E}_{ij} + \frac{\partial P'}{\partial K_{ijk}}\delta\nabla E_{ij} + \frac{\partial P'}{\partial \ddot{K}_{ijk}}\delta\nabla\ddot{E}_{ij} dVdt
\end{aligned}
\tag{A.10}
$$

$$
\begin{aligned}
&Integral_{4a} = \int \frac{\partial P'}{\partial E_{ij}}\delta E_{ij} dVdt = \int \frac{\partial P'}{\partial E_{ij}}\delta U_{i,j} dVdt = \int \left(\frac{\partial P'}{\partial E_{ij}}\delta U_i\right)_{,j} dVdt - \int \nabla_j \left(\frac{\partial P'}{\partial E_{ij}}\right)\delta U_i dVdt \\
&= \int \left(\frac{\partial P'}{\partial E_{ij}}\delta U_i\right) n_j dSdt - \int \frac{\partial}{\partial X_j}\left(\frac{\partial P'}{\partial E_{ij}}\right)\delta U_i dVdt = S_{4a} - \int \frac{\partial}{\partial X_j}\left(\frac{\partial P'}{\partial E_{ij}}\right)\delta U_i dVdt
\end{aligned}
\tag{A.11}
$$

$$Integral_{4b} = \int \frac{\partial P'}{\partial \ddot{E}_{ij}} \delta \ddot{E}_{ij} dVdt = \frac{\partial P'}{\partial \ddot{E}_{ij}} \delta \dot{E}_{ij} \Bigg)_{\Delta T} - \int \frac{\partial}{\partial t}\left(\frac{\partial P'}{\partial \ddot{E}_{ij}} \right) \delta \dot{E}_{ij} dVdt =$$

$$-\frac{\partial}{\partial t}\left(\frac{\partial P'}{\partial \ddot{E}_{ij}} \right) \delta \dot{E}_{ij} \Bigg)_{\Delta T} + \int \frac{\partial^2}{\partial t^2}\left(\frac{\partial P'}{\partial \ddot{E}_{ij}} \right) \delta E_{ij} dVdt$$

$$= \int \frac{\partial^2}{\partial t^2}\left(\frac{\partial P'}{\partial \ddot{E}_{ij}} \right) \delta U_{i,j} dVdt = \int \frac{\partial^2}{\partial t^2}\left(\frac{\partial P'}{\partial \ddot{E}_{ij}} \right) \delta U_i n_j dSdt - \int \frac{\partial}{\partial X_j}\left(\frac{\partial^2}{\partial t^2}\left(\frac{\partial P'}{\partial \ddot{E}_{ij}} \right) \right) \delta U_i dVdt =$$

$$S_{4b} - \int \frac{\partial}{\partial X_j}\left(\frac{\partial^2}{\partial t^2}\left(\frac{\partial P'}{\partial \ddot{E}} \right) \right) \delta U_i dVdt \qquad \text{(A.12)}$$

$$Integral_{4c} = \int \frac{\partial P'}{\partial K_{ijk}} \delta(\nabla E_{ij}) dVdt = \frac{\partial P'}{\partial K_{ijk}} \delta(E_{ij}) \Bigg)_{\Delta T} - \int \frac{\partial}{\partial X_k}\left(\frac{\partial P'}{\partial K_{ijk}} \right) \delta(E_{ij}) dVdt$$

$$= -\int \left(\frac{\partial}{\partial X_k}\left(\frac{\partial P'}{\partial K_{ijk}} \right) \delta U_i n_j dSdt \right) + \int \left(\frac{\partial^2}{\partial X_k \partial X_j}\left(\frac{\partial P'}{\partial K_{ijk}} \right) \delta U_i dVdt \right) \qquad \text{(A.13)}$$

$$= S_{4c} + \int \left(\frac{\partial^2}{\partial X_k \partial X_j}\left(\frac{\partial P'}{\partial K_{ijk}} \right) \delta U_i dVdt \right)$$

$$Integral_{4d} = \int \frac{\partial P'}{\partial \ddot{K}_{ijk}} \delta \nabla \ddot{E}_{ij} dVdt = \frac{\partial P'}{\partial \ddot{K}_{ijk}} \delta \nabla \dot{E}_{ij} \Bigg)_{\Delta T} - \int \frac{\partial}{\partial t}\left(\frac{\partial P'}{\partial \ddot{K}_{ijk}} \right) \delta \nabla \dot{E}_{ij} dVdt$$

$$= -\frac{\partial}{\partial t}\left(\frac{\partial P'}{\partial \ddot{K}_{ijk}} \right) \delta \nabla E_{ij} \Bigg)_{\Delta T} + \int \frac{\partial^2}{\partial t^2}\left(\frac{\partial P'}{\partial \ddot{K}_{ijk}} \right) \delta U_{i,jk} dVdt$$

$$= \int \left(\frac{\partial^2}{\partial t^2}\left(\frac{\partial P'}{\partial \ddot{K}_{ijk}} \right) \delta U_{i,j} \right)_{,k} dVdt - \int \frac{\partial}{\partial X_k}\left(\frac{\partial^2}{\partial t^2}\left(\frac{\partial P'}{\partial \ddot{K}_{ijk}} \right) \right) \delta U_{i,j} dVdt \qquad \text{(A.14)}$$

$$= S_{4d1} - \int \left(\frac{\partial}{\partial X_k}\left(\frac{\partial^2}{\partial t^2}\left(\frac{\partial P'}{\partial \ddot{K}_{ijk}} \right) \right) \delta U_i \right)_{,j} dVdt + \int \frac{\partial^2}{\partial x_j \partial x_k}\left(\frac{\partial^2}{\partial t^2}\left(\frac{\partial P'}{\partial \ddot{K}_{ijk}} \right) \right) \delta U_i dVdt$$

$$= S_{4d1} + S_{4d2} + \int \frac{\partial^2}{\partial X_j \partial X_k}\left(\frac{\partial^2}{\partial t^2}\left(\frac{\partial P'}{\partial \ddot{K}_{ijk}} \right) \right) \delta U_i dVdt$$

$$Integral_5 = \delta \int T'(\dot{E}_{ij}, \nabla \dot{E}_{ij}) dVdt = \int \frac{\partial T'}{\partial \dot{E}_{ij}} \delta \dot{E}_{ij} + \frac{\partial T'}{\partial \dot{K}_{ijk}} \delta \nabla \dot{E}_{ij} dVdt \qquad \text{(A.15)}$$

$$Integral_{5a} = \int \frac{\partial T'}{\partial \dot{E}_{ij}} \delta \dot{E}_{ij} = \frac{\partial T'}{\partial \dot{E}_{ij}} \delta E_{ij} \Bigg)_{\Delta T} - \int \frac{d}{dt}\left(\frac{\partial T'}{\partial \dot{E}_{ij}}\right) \delta E_{ij} dVdt = -\int \frac{d}{dt}\left(\frac{\partial T'}{\partial \dot{E}_{ij}}\right) \delta U_{i,j} dVdt$$
$$= -\int \frac{d}{dt}\left(\frac{\partial T'}{\partial \dot{E}_{ij}}\right) \delta U_i n_j dSdt + \int \frac{\partial}{\partial X_j} \frac{\partial}{\partial t}\left(\frac{\partial T'}{\partial \dot{E}_{ij}}\right) \delta U_i dVdt = S_{5a} + \int \frac{\partial}{\partial X_j} \frac{\partial}{\partial t}\left(\frac{\partial T'}{\partial \dot{E}_{ij}}\right) \delta U_i dVdt \tag{A.16}$$

$$Integral_{5b} = \int \frac{\partial T'}{\partial \dot{K}_{ijk}} \delta \nabla \dot{E}_{ij} dVdt = \int \frac{\partial T'}{\partial \dot{K}_{ijk}} \delta \nabla E_{ij} \Bigg)_{\Delta T} - \int \frac{\partial}{\partial t}\left(\frac{\partial T'}{\partial \dot{K}_{ijk}}\right) \delta \nabla E_{ij} dVdt$$
$$= -\frac{\partial}{\partial t}\left(\frac{\partial T'}{\partial \dot{K}_{ijk}}\right) \delta E_{ij} \Bigg)_{\Delta T} + \int \frac{\partial}{\partial X_k}\left(\frac{\partial}{\partial t}\left(\frac{\partial T'}{\partial \dot{K}_{ijk}}\right)\right) \delta U_{i,j} dVdt$$
$$= \int \frac{\partial}{\partial X_k}\left(\frac{\partial}{\partial t}\left(\frac{\partial T'}{\partial \dot{K}_{ijk}}\right)\right) \delta U_i n_j dVdt - \int \frac{\partial}{\partial X_j}\left(\frac{\partial}{\partial X_k}\left(\frac{\partial}{\partial t}\left(\frac{\partial T'}{\partial \dot{K}_{ijk}}\right)\right)\right) \delta U_i dVdt =$$
$$S_{5b} - \int \frac{\partial}{\partial X_j}\left(\frac{\partial}{\partial X_k}\left(\frac{\partial}{\partial t}\left(\frac{\partial T'}{\partial \dot{K}_{ijk}}\right)\right)\right) \delta U_i dVdt \tag{A.17}$$

Then, inserting (A.4-A.17) back into (A.3) and deriving with respect to time we get the following macro-equation of motion:

$$\int \Sigma_{ij,j} \delta U_i \partial V - \int S_{ijk,jk} \delta U_i dV + \int \frac{\partial}{\partial X_j}\left(\frac{\partial P'}{\partial E_{ij}}\right) \delta U_i dV + \int \frac{\partial}{\partial X_j}\left(\frac{\partial^2}{\partial t^2}\left(\frac{\partial P'}{\partial \ddot{E}_{ij}}\right)\right) \delta U_i dV$$
$$+ \int \frac{\partial}{\partial X_j} \frac{\partial}{\partial t}\left(\frac{\partial T'}{\partial \dot{E}_{ij}}\right) \delta U_i dV - \int \frac{\partial^2}{\partial X_j \partial X_k}\left(\frac{\partial^2}{\partial t^2}\left(\frac{\partial P'}{\partial \ddot{K}_{ijk}}\right)\right) \delta U_i dV - \int \left(\frac{\partial^2}{\partial X_j \partial X_k}\left(\frac{\partial P'}{\partial K_{ij}}\right) \delta U_i dV\right)$$
$$- \int \frac{\partial}{\partial X_j}\left(\frac{\partial}{\partial X_k}\left(\frac{\partial}{\partial t}\left(\frac{\partial T'}{\partial \dot{K}_{ijk}}\right)\right)\right) \delta U_i dV$$
$$-S_1 - S_{2a} - S_{2b} + S_3 - S_{4a} - S_{4b} - S_{4c} - S_{4d1} - S_{4d2} + S_{5a} + S_{5b} = \int \langle \rho \rangle \delta U_i \ddot{U}_i dV \tag{A.18}$$

A.3 Simplification of F_i

In order to simplify the micro-inertia force which is in the last equation of motion (A.18), we use the localization tensors of displacement and for deformation to simplify the form of F_i. Starting with the potential energy P' :

$$P' = -\frac{1}{2}\left\langle \rho\ddot{u}_i \left(u_i - E_{ij}x_j - \frac{1}{2}K_{ijk}x_j x_k \right) \right\rangle$$

$$= -\frac{1}{2}\left\langle \rho\left(H^E_{ijk}\ddot{E}_{jk} + H^K_{ijkl}\ddot{K}_{jkl} \right) \cdot \left(H^E_{imn}E_{mn} + H^K_{imnp}K_{mnp} - E_{im}x_m - \frac{1}{2}K_{imn}x_m x_n \right) \right\rangle$$

$$= -\frac{1}{2}\ddot{E}_{jk}E_{mn}\left\langle \rho H^E_{ijk}H^E_{imn} \right\rangle - \frac{1}{2}\ddot{E}_{jk}K_{mnp}\left\langle \rho H^E_{ijk}H^K_{imnp} \right\rangle + \frac{1}{2}\ddot{E}_{jk}E_{im}\left\langle \rho H^E_{ijk}x_m \right\rangle + \frac{1}{4}\ddot{E}_{jk}K_{imn}\left\langle \rho H^E_{ijk}x_m x_n \right\rangle$$

$$-\frac{1}{2}\ddot{K}_{jkl}E_{mn}\left\langle \rho H^K_{ijkl}H^E_{imn} \right\rangle - \frac{1}{2}\ddot{K}_{jkl}K_{mnp}\left\langle \rho H^K_{ijkl}H^K_{imnp} \right\rangle + \frac{1}{2}\ddot{K}_{jkl}E_{im}\left\langle \rho H^K_{ijkl}x_m \right\rangle + \frac{1}{4}\ddot{K}_{jkl}K_{imn}\left\langle \rho H^K_{ijkl}x_m x_n \right\rangle$$

$$\Rightarrow \frac{\partial^2}{\partial t^2}\left(\frac{\partial P'}{\partial \ddot{E}_{ij}} \right) = -\frac{1}{2}\ddot{E}_{mn}\left\langle \rho H^E_{kij}H^E_{kmn} \right\rangle - \frac{1}{2}\ddot{K}_{mnp}\left\langle \rho H^E_{kij}H^K_{kmnp} \right\rangle + \frac{1}{2}\ddot{E}_{km}\left\langle \rho H^E_{kij}x_m \right\rangle + \frac{1}{4}\ddot{K}_{kmn}\left\langle \rho H^E_{kij}x_m x_n \right\rangle \quad \text{(A.22)}$$

$$\Rightarrow \frac{\partial P'}{\partial E_{ij}} = -\frac{1}{2}\ddot{E}_{mn}\left\langle \rho H^E_{kmn}H^E_{kij} \right\rangle + \frac{1}{2}\ddot{E}_{mn}\left\langle \rho H^E_{imn}x_j \right\rangle - \frac{1}{2}\ddot{K}_{mnl}\left\langle \rho H^K_{kmnl}H^E_{kij} \right\rangle + \frac{1}{2}\ddot{K}_{mkl}\left\langle \rho H^K_{imkl}x_j \right\rangle$$

$$\Rightarrow \frac{\partial^2}{\partial t^2}\left(\frac{\partial P'}{\partial \ddot{K}_{ijk}} \right) = -\frac{1}{2}\ddot{E}_{mn}\left\langle \rho H^K_{lijk}H^E_{lmn} \right\rangle - \frac{1}{2}\ddot{K}_{mnp}\left\langle \rho H^K_{lmnp}H^K_{lijk} \right\rangle + \frac{1}{2}\ddot{E}_{lm}\left\langle \rho H^K_{lijk}x_m \right\rangle + \frac{1}{4}\ddot{K}_{lmn}\left\langle \rho H^K_{lijk}x_m x_n \right\rangle$$

$$\Rightarrow \frac{\partial P'}{\partial K_{ijk}} = -\frac{1}{2}\ddot{E}_{mn}\left\langle \rho H^E_{lmn}H^K_{liik} \right\rangle + \frac{1}{4}\ddot{E}_{mn}\left\langle \rho H^E_{imn}x_j x_k \right\rangle - \frac{1}{2}\ddot{K}_{mnp}\left\langle \rho H^K_{lmnp}H^K_{lijk} \right\rangle + \frac{1}{4}\ddot{K}_{mnp}\left\langle \rho H^K_{imnp}x_j x_k \right\rangle$$

Now we derive the micro-kinetic energy:

$$T' = \left\langle \rho\left(H^E_{ijk}\dot{E}_{jk} + H^K_{ijkl}\dot{K}_{jkl} - \dot{E}_{ij}x_j - \frac{1}{2}\dot{K}_{ijk}x_j x_k \right)\dot{E}_{im}x_m \right\rangle$$

$$+\frac{1}{2}\left\langle \rho\left(H^E_{ijk}\dot{E}_{jk} + H^K_{ijkl}\dot{K}_{jkl} - \dot{E}_{jk}x_k - \frac{1}{2}\dot{K}_{ijk}x_j x_k \right)\dot{K}_{imp}x_m x_p \right\rangle$$

$$+\frac{1}{2}\left\langle \rho\left(H^E_{ijk}\dot{E}_{jk} + H^K_{ijkl}\dot{K}_{jkl} - \dot{E}_{ij}x_j - \frac{1}{2}\dot{K}_{ijk}x_j x_k \right) \cdot \left(H^E_{imp}\dot{E}_{mp} + H^K_{impf}\dot{K}_{mpf} - \dot{E}_{mn}x_n - \frac{1}{2}\dot{K}_{mnp}x_n x_p \right) \right\rangle$$

$$= -\frac{1}{2}\dot{E}_{ij}\dot{E}_{im}\left\langle \rho x_j x_m \right\rangle - \frac{1}{2}\dot{K}_{ijk}\dot{E}_{im}\left\langle \rho x_m x_j x_k \right\rangle - \frac{1}{8}\dot{K}_{ijk}\dot{K}_{imp}\left\langle \rho x_j x_k x_m x_p \right\rangle \quad \text{(A.23)}$$

$$+\frac{1}{2}\dot{E}_{jk}\dot{E}_{mp}\left\langle \rho H^E_{ijk}H^E_{imp} \right\rangle + \dot{K}_{mpf}\dot{E}_{jk}\left\langle \rho H^E_{ijk}H^K_{impf} \right\rangle + \frac{1}{2}\dot{K}_{jkl}\dot{K}_{mpf}\left\langle \rho H^K_{ijkl}H^K_{impf} \right\rangle$$

$$\Rightarrow \frac{\partial}{\partial t}\left(\frac{\partial T'}{\partial \dot{E}_{ij}} \right) = -\ddot{E}_{im}\left\langle \rho x_j x_m \right\rangle - \frac{1}{2}\ddot{K}_{imk}\left\langle \rho x_m x_j x_k \right\rangle + \ddot{E}_{mp}\left\langle \rho H^E_{kij}H^E_{kmp} \right\rangle + \ddot{K}_{mpf}\left\langle \rho H^E_{kij}H^K_{kmpf} \right\rangle$$

$$\Rightarrow \frac{\partial}{\partial t}\left(\frac{\partial T'}{\partial \dot{K}_{ijk}} \right) = -\frac{1}{2}\ddot{E}_{im}\left\langle \rho x_m x_j x_k \right\rangle - \frac{1}{4}\ddot{K}_{imp}\left\langle \rho x_m x_j x_k x_p \right\rangle + \ddot{E}_{pf}\left\langle \rho H^E_{mpf}H^K_{mijk} \right\rangle + \ddot{K}_{mpf}\left\langle \rho H^K_{lijk}H^K_{lmpf} \right\rangle$$

After deriving the kinetic and potential energy, we insert these expressions into the last expression of Fi as the following:

$$F_i = \frac{\partial}{\partial X_j}\left(\frac{1}{2}\ddot{E}_{mn}\left\langle\rho\left(H^E_{imn}x_j + H^E_{mij}x_n - 2\delta^m_i x_j x_n\right)\right\rangle + \frac{1}{2}\ddot{K}_{rst}\left\langle\rho\left(H^K_{irst}x_j + \frac{1}{2}H^E_{rij}x_s x_t - \delta^r_i x_s x_j x_t\right)\right\rangle\right)$$
$$-\frac{\partial^2}{\partial X_j \partial X_k}\left(\begin{array}{l}\ddot{E}_{pq}\left\langle\frac{\rho}{2}\left(H^K_{pijk}x_q + \frac{1}{2}H^E_{ipq}x_j x_k - \delta^p_i x_q x_j x_k\right)\right\rangle \\ +\frac{1}{4}\ddot{K}_{rst}\left\langle\rho\left(H^K_{rijk}x_s x_t + H^K_{irst}x_j x_k - \delta^r_i x_s x_j x_k x_t\right)\right\rangle\end{array}\right) \qquad \text{(A.24)}$$

Appendix B: High gradient dynamic homogenization method

Using the definition of internal energy, we expand it in function of the localization tensors:

$$\begin{aligned}
&2.W^{\text{int}}(E,K) = \left(E_{ij}.\Sigma_{ij} + K_{ijk}.S_{ijk}\right) = \left\langle\varepsilon_{ij}\sigma_{ij}\right\rangle + \left\langle\rho\ddot{u}_i\left(u_i - E_{ij}x_j - \frac{1}{2}K_{ijk}x_j x_k\right)\right\rangle \\
&= \left\langle\left(A^E_{ijkl}.E_{kl} + A^K_{ijklf}.K_{klf}\right).C_{ijmn}.\left(A^E_{mnrs}.E_{rs} + A^K_{mnrst}K_{rst}\right)\right\rangle \\
&+\left\langle\rho\left(H^E_{ijk}.\ddot{E}_{jk} + H^K_{ijkl}.\ddot{K}_{jkl}\right).\left(H^E_{iqr}.E_{qr} + H^K_{irst}.K_{rst} - E_{iq}x_q - \frac{1}{2}K_{iqr}x_q x_r\right)\right\rangle \\
&= \left\langle A^E_{ijkl}E_{kl}.C_{ijmn}.A^E_{mnrs}.E_{rs} + A^E_{ijkl}.E_{kl}C_{ijmn}A^K_{mnrst}K_{rst} + A^K_{ijklf}K_{klf}C_{ijmn}A^E_{mnrs}E_{rs} + A^K_{ijklf}K_{klf}C_{ijmn}A^K_{mnrst}K_{rst}\right\rangle \\
&+\left\langle\rho\left(\begin{array}{l}H^E_{ijk}\ddot{E}_{jk}H^E_{iqr}E_{qr} + H^E_{ijk}\ddot{E}_{jk}H^K_{irst}K_{rst} - H^E_{ijk}\ddot{E}_{jk}E_{iq}x_q - \frac{1}{2}H^E_{ijk}\ddot{E}_{jk}K_{iqr}x_q x_r \\ +H^K_{ijkl}\ddot{K}_{jkl}H^E_{iqr}E_{qr} + H^K_{ijkl}\ddot{K}_{jkl}H^K_{irst}K_{rst} - H^K_{ijkl}\ddot{K}_{jkl}E_{iq}x_q - \frac{1}{2}H^K_{ijkl}\ddot{K}_{jkl}K_{iqr}x_q x_r\end{array}\right)\right\rangle
\end{aligned} \qquad \text{(B.1)}$$

The macroscopic stress is the variation of the internal energy with respect to the macro-deformation:

$$\Sigma^{dyn}{}_{ij} = \frac{\partial W^{\text{int}}(E,K,\ddot{E},\ddot{K})}{\partial E_{ij}} + \frac{\partial^2}{\partial t^2}\left(\frac{\partial W^{\text{int}}(E,K,\ddot{E},\ddot{K})}{\partial \ddot{E}_{ij}}\right)$$

$$= \frac{1}{2}\left\langle \begin{array}{l} A^E_{klij}.C_{klmn}.A^E_{mnrs}.E_{rs} + A^E_{rskl}.C_{rsmn}.A^E_{mnij}.E_{kl} + A^E_{klij}.C_{klmn}.A^K_{mnrst}.K_{rst} + A^K_{rsklf}K_{klf}C_{rsmn}A^E_{mnij} \\ +\rho H^E_{qrk}\ddot{E}_{rk}H^E_{pij} - \rho H^E_{iqk}\ddot{E}_{qk}x_j + \rho H^K_{qrkl}\ddot{K}_{rkl}H^E_{qij} - \rho H^K_{iqkl}\ddot{K}_{qkl}x_j + \rho H^E_{kij}\ddot{E}_{qr}H^E_{kqr} \\ +\rho H^K_{krst}\ddot{K}_{rst}H^E_{kij} - \rho H^E_{kij}\ddot{E}_{kq}x_q - \frac{1}{2}\rho\ddot{K}_{kqr}H^E_{kij}x_q x_r \end{array}\right\rangle \qquad \text{(B.2)}$$

$$\Sigma^{dyn}{}_{ij} = E_{dl}\left\langle\frac{1}{2}\left(A^E_{krij}C_{krmn}A^E_{mndl} + A^E_{rsdl}.C_{rsmn}.A^E_{mnij}\right)\right\rangle + K_{rst}\left\langle\frac{1}{2}\left(A^E_{klij}C_{klmn}A^K_{mnrst} + A^K_{klrst}C_{klmn}A^E_{mnij}\right)\right\rangle$$

$$+\ddot{E}_{dl}\left\langle\frac{\rho}{2}\left(H^E_{qdl}H^E_{qij} + H^E_{kij}H^E_{kdl} - H^E_{idl}x_j - H^E_{dij}x_l\right)\right\rangle$$

$$+\ddot{K}_{rst}\left\langle\frac{\rho}{2}\left(H^K_{qrst}H^E_{qij} + H^K_{krst}H^E_{kij} - H^K_{irst}x_j - \frac{1}{2}H^E_{rij}x_s x_t\right)\right\rangle$$

The hyper-stress is also the variation of the internal energy with respect to the second gradient deformation:

$$S_{ijk} = \frac{\partial W^{\text{int}}(E,K,\ddot{E},\ddot{K})}{\partial K_{ijk}} + \frac{\partial^2}{\partial t^2}\frac{\partial W^{\text{int}}(E,K,\ddot{E},\ddot{K})}{\partial \ddot{K}_{ijk}}$$

$$= \frac{1}{2}\left\langle \begin{array}{l} A^E_{rstl}E_{tl}C_{rsmn}A^K_{mnijk} + A^K_{rsijk}C_{rsmn}A^E_{mndl}E_{dl} + A^K_{rsijk}C_{rsmn}A^K_{mndlt}K_{dlt} \\ +A^K_{rstlf}C_{rsmn}A^K_{mnijk}K_{tlf} + \rho H^E_{rst}\ddot{E}_{st}H^K_{rijk} - \frac{1}{2}\rho H^E_{iqr}\ddot{E}_{qr}x_k x_j \\ +\rho H^E_{lqr}\ddot{E}_{qr}H^K_{lijk} + \rho H^K_{lijk}H^K_{lrst}\ddot{K}_{rst} + \rho H^K_{dstl}H^K_{dijk}\ddot{K}_{stl} \\ -\rho\ddot{E}_{lq}H^K_{lijk}x_l - \frac{1}{2}\rho H^K_{lijk}K_{lqr}x_q x_r - \frac{1}{2}\rho H^K_{iqrl}K_{qrl}x_j x_k \end{array}\right\rangle \qquad \text{(B.3)}$$

$$S_{ijk} = \left\langle\frac{1}{2}A^E_{rsdl}C_{rsmn}A^K_{mnijk} + \frac{1}{2}A^K_{rsijk}C_{rsmn}A^E_{mndl}\right\rangle.E_{dl} + \left\langle\frac{1}{2}A^K_{pfijk}C_{pfmn}A^K_{mnrst} + \frac{1}{2}A^K_{dlrst}C_{dlmn}A^K_{mnijk}\right\rangle.K_{rst}$$

$$+\left\langle\frac{\rho}{2}\left(H^E_{qdl}H^K_{qijk} + H^E_{rdl}H^K_{rijk} - \frac{1}{2}H^E_{idl}x_k x_j - H^K_{dijk}x_l\right)\right\rangle.\ddot{E}_{dl} +$$

$$\left\langle\frac{\rho}{2}\left(H^K_{lrst}H^K_{lijk} + H^K_{drst}H^K_{dijk} - \frac{1}{2}H^K_{rijk}x_s x_t - \frac{1}{2}H^K_{irst}x_j x_k\right)\right\rangle.\ddot{K}_{rst}$$

Appendix C: Elasticity Solution

Using the elasticity theory and Floquet's theorem (Sun et al., 1968) they derive the exact dispersion relation of the longitudinal wave propagating in the direction normal to the layering (C.1) as follows:

$$\cos\left(k\left(d_f + d_m\right)\right) = \cos\left(kd_m \frac{c}{c_L^m}\right)\cos\left(kd_f \frac{c}{c_L^f}\right) - \left[\frac{\left(1+p^2\right)}{2p}\right]\sin\left(kd_m \frac{c}{c_L^m}\right)\sin\left(kd_f \frac{c}{c_L^f}\right) \tag{C.1}$$

where $p = \dfrac{\left(\lambda_f + 2\mu_f\right)c_L^m}{\left(\lambda_m + 2\mu_m\right)c_L^f}$

The dispersion of the transverse wave propagating in the direction normal to the layering will be obtained by replacing in (C.1) $\left(\lambda_f + 2\mu_f\right)$ by $2\mu_f$ and $\left(\lambda_m + 2\mu_m\right)$ by $2\mu_m$ respectively.